

Microscopic theory of multiple-phonon-mediated dephasing and relaxation of quantum dots near a photonic band gap

Chiranjeeb Roy and Sajeev John*

Department of Physics, University of Toronto, Toronto, Ontario M5S 1A7, Canada

(Received 12 June 2009; revised manuscript received 9 December 2009; published 18 February 2010)

We derive a quantum theory of the role of acoustic and optical phonons in modifying the optical absorption line shape, polarization dynamics, and population dynamics of a two-level atom (quantum dot) in the “colored” electromagnetic vacuum of a photonic band-gap (PBG) material. This is based on a microscopic Hamiltonian describing both radiative and vibrational processes quantum mechanically. We elucidate the extent to which phonon-assisted decay limits the lifetime of a single photon-atom bound state and derive the modified spontaneous emission dynamics due to coupling to various phonon baths. We demonstrate that coherent interaction with undamped phonons can lead to an enhanced lifetime of a photon-atom bound state in a PBG. This results in reduction of the steady-state atomic polarization but an increase in the fractionalized upper state population in the photon-atom bound state. We demonstrate, on the other hand, that the lifetime of the photon-atom bound state in a PBG is limited by the lifetime of phonons due to lattice anharmonicities (breakup of phonons into lower energy phonons) and purely nonradiative decay. We also derive the modified polarization decay and dephasing rates in the presence of such damping. This leads to a microscopic, quantum theory of the optical absorption line shapes. Our model and formalism provide a starting point for describing dephasing and relaxation in the presence of external coherent fields and multiple quantum dot interactions in electromagnetic reservoirs with radiative memory effects.

DOI: [10.1103/PhysRevA.81.023817](https://doi.org/10.1103/PhysRevA.81.023817)

PACS number(s): 42.70.Qs, 32.80.–t

I. INTRODUCTION

Recent advances in the synthesis of ultra-high quality photonic crystals and three-dimensional (3D) photonic band-gap (PBG) materials suggest the possibility of observing engineered atom-photon interactions in these systems. One of the most dramatic consequences of light localization [1,2] in PBG materials is the inhibition of spontaneous emission of light from atoms [3,4] and the formation of the photon-atom bound state [5–9]. When the atomic resonance lies very close to a photonic band edge or other sharp features in the electromagnetic density of states, the radiative dynamics can exhibit long time memory (non-Markovian) effects. Important new phenomenon such as the ability to population-invert a two-level system by coherently pumping on resonance is possible [10–15]. Many of the effects rely on the microfabrication of PBG materials with resolution on the scale of a few nanometers in the vicinity of a quantum dot. Other applications of the photon-atom bound state to quantum information processing further rely on the ability to deter nonradiative relaxation and decoherence channels. Experimental studies of quantum entanglement of photons propagating through photonic crystals have recently been initiated [16]. In light of these developments, it is timely to consider the role of phonon-mediated relaxation and decoherence of optically excited quantum dots in photonic crystals from a microscopic point of view.

For quantum dots, the role of phonons in polarization relaxation is very important [17–21]. For instance, high-resolution photoluminescence spectra of single quantum dots show a narrow zero-phonon line on top of a broad background. The background can be attributed to acoustic phonons [22].

In this work, we develop and analyze a microscopic model of phonons in modifying the spectral characteristics of a quantum dot in a photonic crystal. Starting from a complete microscopic Hamiltonian describing the dot-exciton, photon, and phonon degrees of freedom, we derive the quantum dynamics of the system at a finite temperature. This provides a more fundamental picture of excited state population, atomic polarization, and spectral line shape than previous studies [23–28]. Our microscopic theory then enables a description of damped (anharmonic) phonon contributions to non-Markovian atom-radiation field interaction and the stability of the photon-atom bound state.

The theory developed in this article is relevant to self-assembled $\text{In}_x\text{Ga}_{x-1}\text{As}/\text{GaAs}$ quantum dots where phonon-induced dephasing can be described by the Independent-Boson model [17]. Here, an epitaxial layer of $\text{In}_x\text{Ga}_{x-1}\text{As}$ grown on a substrate of GaAs has a reduction in the strain energy due to lattice mismatch. This leads to quantum dot formation by the breaking up of the growing layer into small clumps. Experimental studies [29–31] in strongly confined quantum dots at low temperatures have clearly demonstrated that the polarization decay has a non-Lorentzian homogenous line shape with a very narrow zero-phonon line superimposed on a broad acoustic-phonon spectrum. These $\text{In}_x\text{Ga}_{x-1}\text{As}/\text{GaAs}$ quantum dot excitons have lifetimes as long as $T_1 = 900$ ps in an unstructured electromagnetic vacuum with dephasing times $T_2 = 630$ ps at cryogenic temperatures [32–34]. Since the dephasing times are almost as large as the decay times, dephasing in these materials is radiatively limited. The exciton lifetime can be extended by placing these quantum dots inside the structured electromagnetic reservoir of the photonic crystal such that the radiative recombination of the electrons and the holes is suppressed by a photonic band gap. It is interesting to experimentally study the effects of suppression of radiative recombination resulting in much larger exciton

*john@physics.utoronto.ca

lifetimes. In this regime, pure dephasing (interaction with undamped phonons) is an important effect. We also extend the effects of phonon induced dephasing beyond the Independent-Boson model by introducing, phenomenologically, a finite lifetime for the phonons themselves. Direct nonradiative decay of the two-level system is also considered. This leads to population and polarization decay due to phonons in addition to electromagnetic dephasing and relaxation.

The outline of this article is as follows. In Sec. II, we introduce a model Hamiltonian that simultaneously describes the radiative and nonradiative quantum processes leading to dephasing and decoherence of a two-level system. We derive an effective Hamiltonian using mean-field theory. In this approximation, the effective dipole-moment incorporates the mean-field response of the lattice and is temperature dependent. We demonstrate that this mean-field theory captures the absorption and emission spectra arising from phonon sidebands in a general photonic reservoir. We then develop a theory to calculate the polarization dynamics and the lifetime of the two-level system in the presence of phonons. In Sec. IV, we apply our theory to a quantum dot placed inside a photonic crystal. We first study the absorption line shape and show that phonon-mediated sidebands can lead to absorption of photons inside the photonic band gap. We then calculate the polarization and excitation probability of the two-level atom and show that for long phonon lifetimes the atom can have some residual coherence even at large times. This residual coherence is a consequence of the fractionalized steady-state due to the formation of the photon-atom bound state. In Sec. V, we discuss the role of acoustic phonon-induced dephasing on the polarization dynamics and population decay. We then generalize our Hamiltonian to allow for nonradiative decay processes. This enables us to extend our theory beyond pure dephasing. We also discuss the loss of coherence and decay of the photon-atom bound state due to phonon-phonon scattering and other anharmonic processes (finite phonon lifetime) [35]. Finally, in Sec. VI, we present our conclusions.

II. MODEL HAMILTONIAN FOR THE DOT-PHOTON-PHONON SYSTEM

It is well known that nonradiative exciton decay in quantum dots caused by phonons can be suppressed due to quantization effects [36,37]. For instance, in a bulk medium with nearly dispersionless longitudinal-optical (LO) phonons, purely nonradiative decay requires the exciton recombination energy to be an integer multiple of LO phonon energies. This resonance condition leads to the phonon-bottleneck effect. In a photonic crystal environment, in which quantum dots are embedded in periodic array of sub-micron-scale dielectric rods, such bottlenecks may apply to acoustic phonons as well. Quantum confinement in the quantum dot increases the coupling of electrons to short-wavelength phonons. This strengthens multiple phonon-assisted absorption and emission processes. Phonon sidebands exist for both acoustic and optical phonons. Optical phonons give rise to discrete sidebands separated by the optical phonon energy. Acoustic phonons in a bulk medium occupy a broad continuum of energies and give rise to significant line broadening.

We consider a quantum dot (two-level system) with level separation much larger than all phonon energies so that phonon-induced mixing of different electronic levels can be neglected. The full Hamiltonian of our dot exciton, phonon, and photon system can be written as $H = H_0 + H_I$, where

$$H_0 = \hbar\omega_0\hat{\sigma}_{ee} + \sum_k \hbar\omega_k\hat{a}_k^\dagger\hat{a}_k + \sum_q \hbar\Omega_q\hat{c}_q^\dagger\hat{c}_q, \quad (1a)$$

$$H_I = \sum_k (\lambda_k\hat{\sigma}_{eg}\hat{a}_k + \lambda_k^*\hat{a}_k^\dagger\hat{\sigma}_{ge}) + \hat{\sigma}_{ee} \sum_q \eta_q(\hat{c}_q + \hat{c}_q^\dagger), \quad (1b)$$

where $\hat{\sigma}_{eg}(\hat{\sigma}_{ge})$ is the raising (lowering) operator for the two-level atom, $\hat{c}_q^\dagger(\hat{c}_q)$ is the creation (annihilation) operator for the phonon with wave number q , and $\hat{a}_k^\dagger(\hat{a}_k)$ is the creation (annihilation) operator for the photon. λ_k and η_q are exciton-photon and exciton-phonon coupling parameters, respectively. ω_0 is the resonant frequency of the two-level atom, and Ω_q and ω_k are the phonon and photon dispersion relations, respectively. The two-level atom operators obey the commutation relation:

$$[\hat{\sigma}_{ij}, \hat{\sigma}_{kl}] = \delta_{jk}\hat{\sigma}_{il} - \delta_{il}\hat{\sigma}_{kj}. \quad (2)$$

The photon and phonon operators obey bosonic commutation relations: $[\hat{a}_k, \hat{a}_{k'}^\dagger] = \delta(k - k')$ and $[\hat{c}_q, \hat{c}_{q'}^\dagger] = \delta(q - q')$. In the absence of dot-photon coupling ($\lambda_k = 0$), the Hamiltonian Eq. (1) reduces to the Independent-Boson model used in the literature [17] to study pure dephasing of two-level systems coupled to a phonon bath.

Optical interaction with quantum dots in a smooth, featureless electromagnetic reservoir can be treated in the standard Fermi Golden Rule framework. However, in the ‘‘colored vacuum’’ of a photonic crystal, abrupt changes in the photon density of states (with frequency) introduce non-Markovian memory effects [38] in the quantized electromagnetic field. The resonant interaction of the two-level system with the quantized electromagnetic field is written in a rotating wave approximation, where the dot-photon coupling constant is given by [39]

$$\lambda_k = i \frac{\omega_0 |\vec{D}_{ge}|}{\hbar} \left(\frac{\hbar}{2\epsilon_0 \omega_k V} \right)^{\frac{1}{2}} \vec{e}_k \cdot \vec{u}_d. \quad (3)$$

Here, the atomic dipole moment $|\vec{D}_{ge}|$ has been chosen to be real and \vec{u}_d is a unit vector parallel to $|\vec{D}_{ge}|$. The vector \vec{e}_k is the transverse polarization unit vector of the radiation field, and V is the quantization (sample) volume.

The interaction of the electron with phonons both shifts the exciton recombination energy and leads to scattering effects. In order to isolate the overall energy shift, we use the (canonical) polaron-transformation:

$$\tilde{H} = \exp(S)H \exp(-S), \quad (4a)$$

where

$$S = \hat{\sigma}_{ee} \sum_q \frac{\eta_q}{\Omega_q} (\hat{c}_q^\dagger - \hat{c}_q). \quad (4b)$$

For convenience we choose units such that $\hbar = 1$. The canonical transformation diagonalizes the Hamiltonian Eq. (1)

to the form $\tilde{H} = \tilde{H}_0 + H_p$, where

$$\tilde{H}_0 = (\omega_0 - \Delta)\hat{\sigma}_{ee} + \sum_k \omega_k \hat{a}_k^\dagger \hat{a}_k + \sum_k (\lambda_k \hat{C}_+ \hat{\sigma}_{eg} \hat{a}_k + \lambda_k^* \hat{a}_k^\dagger \hat{C}_- \hat{\sigma}_{ge}), \quad (5a)$$

$$H_p = \sum_q \Omega_q \hat{c}_q^\dagger \hat{c}_q. \quad (5b)$$

Here we have introduced a lattice displacement operator:

$$\hat{C}_\pm = \exp \left[\pm \sum_q \frac{\eta_q}{\Omega_q} (\hat{c}_q^\dagger - \hat{c}_q) \right] \quad (6a)$$

and

$$\Delta = \sum_q \frac{\eta_q^2}{\Omega_q}. \quad (6b)$$

Δ is called the polaron shift and accounts for the renormalization of the resonant frequency of the two-level atom due to phonon emission and reabsorption.

A mean-field theory of the electron-thermal lattice vibration interaction is obtained by replacing \hat{C}_+ and \hat{C}_- by their thermal expectation values $\langle \hat{C}_+ \rangle$ and $\langle \hat{C}_- \rangle$ evaluated with respect to the pure phonon Hamiltonian H_p [40]

$$\begin{aligned} \langle \hat{C}_\pm \rangle &= \frac{\text{Tr}[\exp(-\beta H_p) \hat{C}_\pm]}{\text{Tr}[\exp(-\beta H_p)]} \\ &= \exp \left[-\frac{1}{2} \sum_q \frac{\eta_q^2}{\Omega_q^2} (1 + 2\langle \hat{c}_q^\dagger \hat{c}_q \rangle) \right]. \end{aligned} \quad (7)$$

The mean-field decomposition we use in this article also has been considered by Anda and Ure [41] in the context of chemisorption of hydrogen. As we show, this approximation can be used to recapture important features of the exciton line shape caused by multiphonon absorption and emission sidebands. The thermal averages of the phonon operators are evaluated assuming that the phonon bath is at thermal equilibrium at temperature T and $\beta = 1/k_B T$. The Hamiltonian Eq. (5) is simplified to

$$H_{MF} = (\omega_0 - \Delta)\hat{\sigma}_{ee} + \sum_k \omega_k \hat{a}_k^\dagger \hat{a}_k + \sum_k (\tilde{\lambda}_k \hat{\sigma}_{eg} \hat{a}_k + \tilde{\lambda}_k^* \hat{a}_k^\dagger \hat{\sigma}_{ge}), \quad (8)$$

where $\tilde{\lambda}_k = \lambda_k \langle \hat{C}_+ \rangle$ and $\tilde{\lambda}_k^* = \lambda_k^* \langle \hat{C}_- \rangle$. This mean-field approximation relies on the separation of time scales between optical and vibrational processes for realistic systems in which $\lambda_k \ll \eta_q$. Since $\hbar/\lambda_k \gg \hbar/\eta_q$, phonon scattering occurs very rapidly compared with purely radiative processes. In other words, the dot-phonon system can reach equilibrium quickly in response to any slow change arising from radiative processes.

III. OPTICAL SUSCEPTIBILITY AND LINE SHAPE

A. Absorption line shape

We begin by deriving a general formalism to calculate the absorption line shape and the rate of decay of an exciton coupled to a general photonic and a thermal phonon reservoir.

The absorption line shape $\chi_a(\omega)$ is related to the two-time dipole correlation function [42]:

$$\chi_a(\omega) = \frac{iN_d}{\epsilon_0 \hbar} \int_{-\infty}^{\infty} dt \Theta(t) \exp(i\omega t) \langle [\hat{d}(t), \hat{d}(0)] \rangle, \quad (9)$$

where the angular brackets denote thermodynamic averages and $\hat{d}(t) = \exp(iHt)\hat{d}(0)\exp(-iHt)$ with H defined in Eq. (1) and the dipole operator \hat{d} defined in the following discussion. Also, N_d is the number of dipoles in a unit volume. The step function $\Theta(t)$ is defined by $\Theta(t) = 1$ for $t \geq 0$ and $\Theta(t) = 0$ otherwise.

The susceptibility $\chi_a(\omega)$ describes the linear response of a two-level atom placed in a normalization volume V to an external field of frequency ω . The dipole moment operator \hat{d} of an isotropic two-level system is given by $\hat{d} = |D_{ge}|(\hat{\sigma}_{ge} + \hat{\sigma}_{eg})$, where $|D_{ge}|$ is the transition dipole moment connecting the ground($|g\rangle$) and the excited($|e\rangle$) states. It is useful to express the susceptibility in terms of the thermodynamic Green's functions of the dipole operators as follows:

$$\begin{aligned} \chi_a(\omega) &= -\frac{N_d}{\epsilon_0 \hbar} |D_{ge}|^2 \lim_{\epsilon \rightarrow 0} [G_{\omega+i\epsilon}(\hat{\sigma}_{ge}; \hat{\sigma}_{eg}) + G_{\omega+i\epsilon}(\hat{\sigma}_{eg}; \hat{\sigma}_{ge}) \\ &\quad + G_{\omega+i\epsilon}(\hat{\sigma}_{eg}; \hat{\sigma}_{eg}) + G_{\omega+i\epsilon}(\hat{\sigma}_{ge}; \hat{\sigma}_{ge})], \end{aligned} \quad (10)$$

where $G_\omega(\hat{A}; \hat{B}) = -i \int_{-\infty}^{\infty} dt e^{i\omega t} \Theta(t) [\hat{A}(t), \hat{B}(0)]$ [43,44]. The infinitesimal imaginary part ϵ is added to shift the poles of $\chi(\omega)$ to the lower half of the complex ω plane. The susceptibility $\chi_a(\omega)$ is well defined for positive and negative frequencies. Using the properties of a thermodynamic Green's function $G_{\omega+i\epsilon}(\hat{\sigma}_{eg}; \hat{\sigma}_{ge})$ can be calculated from $G_{\omega+i\epsilon}(\hat{\sigma}_{ge}; \hat{\sigma}_{eg})$ by substituting ω with $-\omega$. Moreover $G_{\omega+i\epsilon}(\hat{\sigma}_{eg}; \hat{\sigma}_{eg})$ and $G_{\omega+i\epsilon}(\hat{\sigma}_{ge}; \hat{\sigma}_{ge})$ are zero. In the following, we focus on the evaluation of $G_{\omega+i\epsilon}(\hat{\sigma}_{ge}; \hat{\sigma}_{eg})$ in the expression for optical susceptibility Eq. (10).

Consider the Green's function in the time domain

$$\begin{aligned} G_t(\hat{\sigma}_{ge}; \hat{\sigma}_{eg}) &= -i\Theta(t) \langle [\hat{\sigma}_{ge}(t), \hat{\sigma}_{eg}(0)] \rangle_H \\ &= -i\Theta(t) \langle \langle e^{iHt} \hat{\sigma}_{ge} e^{-iHt} \hat{\sigma}_{eg} \rangle \rangle_H \\ &\quad - \langle \hat{\sigma}_{eg} e^{iHt} \hat{\sigma}_{ge} e^{-iHt} \rangle_H, \end{aligned} \quad (11)$$

where the correlation functions are evaluated in thermodynamic equilibrium with respect to the full Hamiltonian Eq. (1). Here and throughout the rest of this article, we use units in which $\hbar = 1$. Using the fact that the trace is invariant under unitary transformations, we get

$$\begin{aligned} G_t(\hat{\sigma}_{ge}; \hat{\sigma}_{eg}) &= \tilde{G}_t(\hat{\sigma}_{ge}; \hat{\sigma}_{eg}) \\ &= -i\Theta(t) \langle \langle e^{i\tilde{H}t} \hat{\sigma}_{ge} e^{-i\tilde{H}t} \hat{\sigma}_{eg} \rangle \rangle_{\tilde{H}} \\ &\quad - \langle \hat{\sigma}_{eg} e^{i\tilde{H}t} \hat{\sigma}_{ge} e^{-i\tilde{H}t} \rangle_{\tilde{H}}, \end{aligned} \quad (12)$$

where \tilde{H} is the polaron-transformed Hamiltonian defined in Eq. (5), $\hat{\sigma}_{ge} = \exp(S)\hat{\sigma}_{ge}\exp(-S) = \hat{\sigma}_{ge}\hat{C}_-$, $\hat{\sigma}_{eg} = \exp(S)\hat{\sigma}_{eg}\exp(-S) = \hat{\sigma}_{eg}\hat{C}_+$, $S = \hat{\sigma}_{ee} \sum_q \frac{\eta_q}{\Omega_q} (\hat{c}_q^\dagger - \hat{c}_q)$, and \hat{C}_\pm are defined in Eq. (6). The trace can be evaluated in a closed form in a mean-field approximation that replaces \tilde{H} with $H_{MF} + H_p$. With respect to the Hamiltonian Eq. (8), we

have

$$\begin{aligned} \tilde{G}_t^{MF}(\hat{\sigma}_{ge}; \hat{\sigma}_{eg}) &= -i\Theta(t) \langle (e^{iH_{MF}t} \hat{\sigma}_{ge} e^{-iH_{MF}t} \hat{\sigma}_{eg})_{H_{MF}} \rangle \\ &\times \langle e^{iH_p t} \hat{C}_- e^{-iH_p t} \hat{C}_+ \rangle_{H_p} - \langle \hat{\sigma}_{eg} e^{iH_{MF}t} \hat{\sigma}_{ge} e^{-iH_{MF}t} \rangle_{H_{MF}} \\ &\times \langle \hat{C}_+ e^{iH_p t} \hat{C}_- e^{-iH_p t} \rangle_{H_p}, \end{aligned} \quad (13)$$

where $\tilde{G}_t^{MF}(\hat{\sigma}_{ge}; \hat{\sigma}_{eg})$ is the Green's function calculated with respect to the polaron-transformed mean-field Hamiltonian Eq. (8) plus the phonon Hamiltonian Eq. (5b). The thermal averages over the phonon modes are well known and are given by [40]

$$\langle \hat{C}_\pm(t) \hat{C}_\mp(0) \rangle_{H_p} = e^{-[\Phi(0) - \Phi(t)]}, \quad (14a)$$

$$\langle \hat{C}_\pm(0) \hat{C}_\mp(t) \rangle_{H_p} = e^{-[\Phi(0) - \Phi(-t)]}, \quad (14b)$$

where $\Phi(t)$ is given by

$$\Phi(t) = \sum_q \frac{\eta_q^2}{\Omega_q^2} [N_q \exp(i\Omega_q t) + (N_q + 1) \exp(-i\Omega_q t)] \quad (15)$$

and $N_q = \langle \hat{c}_q^\dagger \hat{c}_q \rangle = (\exp(\beta\Omega_q) - 1)^{-1}$. From Eq. (7), we see that (we have dropped the subscript H_p on the thermal averages)

$$\langle \hat{C}_\pm \rangle \langle \hat{C}_\pm \rangle = \exp\left(-\sum_q \frac{\eta_q^2}{\Omega_q^2} (1 + 2N_q)\right) = e^{-\Phi(0)}. \quad (16)$$

For illustration purposes, we now consider the Einstein model of dispersionless phonons [40]. In this case, $\Phi(t)$ is given by

$$\Phi(t) = g[N \exp(i\Omega_0 t) + (N + 1) \exp(-i\Omega_0 t)], \quad (17)$$

where $g = \sum_q \frac{\eta_q^2}{\Omega_0^2}$ and $N = \frac{1}{\exp(\beta\Omega_0) - 1}$ is the number of thermally excited optical phonons.

If the equilibrium temperature of the two-level system interacting with the photon reservoir is assumed to be very low compared with the two-level transition frequency, one can easily show [45]

$$\tilde{G}_t^{MF}(\hat{\sigma}_{ge}; \hat{\sigma}_{eg}) \simeq G_t^{MF}(\hat{\sigma}_{ge}; \hat{\sigma}_{eg}) e^{-[\Phi(0) - \Phi(t)]} \quad (t > 0). \quad (18)$$

Expanding $\exp\{-[\Phi(0) - \Phi(t)]\}$ in a power series in $\exp(i\Omega_0 t)$, it can be shown [40] that the Green's function has the form

$$\tilde{G}_\omega^{MF}(\hat{\sigma}_{ge}; \hat{\sigma}_{eg}) = \sum_{n=-\infty}^{\infty} L_n G_{\omega-n\Omega_0}^{MF}(\hat{\sigma}_{ge}; \hat{\sigma}_{eg}) \quad (t > 0), \quad (19)$$

where

$$L_n = e^{-g(2N+1)} e^{n\Omega_0\beta/2} I_n[2g\sqrt{N(N+1)}] \quad (20)$$

and $I_n(z)$ is the n th-order modified-Bessel function of the first kind with complex argument z . Here we have made use of the relation $\sqrt{(N+1)/N} = e^{\frac{\beta\Omega_0}{2}}$ as well as of the identity [46] $e^{z\cos(\theta)} = \sum_{n=-\infty}^{\infty} I_n(z) e^{in\theta}$. The n th term in this infinite series represents the net change in phonon number during an optical transition. For $n \geq 1$, this corresponds to phonon-assisted optical transitions where n more phonons are emitted than absorbed by the quantum dot into the phonon reservoir. Analogous results can be derived for dispersive phonon models (e.g., acoustic phonons). However, a simple power series expansion of the acoustic phonon Green's function cannot be made and recourse must be made to numerical methods.

In order to simplify the notation, we denote $G_{\omega-n\Omega_0}^{MF}(\hat{\sigma}_{ge}; \hat{\sigma}_{eg}) \equiv G_{\omega,n}^{MF}(\hat{\sigma}_{ge}; \hat{\sigma}_{eg})$. It is easy to see that $G_{\omega,n}^{MF}(\hat{\sigma}_{ge}; \hat{\sigma}_{eg})$ satisfies the equation of motion:

$$\begin{aligned} (\omega - n\Omega_0) G_{\omega,n}^{MF}(\hat{\sigma}_{ge}; \hat{\sigma}_{eg}) &= \langle [\hat{\sigma}_{ge}(0), \hat{\sigma}_{eg}(0)] \rangle_{H_{MF}} + G_{\omega,n}^{MF}([\hat{\sigma}_{ge}, H_{MF}], \hat{\sigma}_{eg}). \end{aligned} \quad (21)$$

The first term on the right-hand side is equal to unity in thermal equilibrium since $\langle \hat{\sigma}_{gg} \rangle \simeq 1$ and $\langle \hat{\sigma}_{ee} \rangle \simeq 0$ for $\hbar\omega_0 \gg k_B T$. The corresponding equation of motion for $G_{\omega,n}^{MF}([\hat{\sigma}_{ge}, H_{MF}], \hat{\sigma}_{eg})$ leads to a hierarchy of equations involving higher order correlation functions. This hierarchy can be closed by decoupling certain photon correlation functions from atomic correlation functions. Physically, this decoupling scheme corresponds to neglecting multiphoton processes and considering only temperatures very low compared with the quantum dot transition energy scale. On the other hand, multiphonon processes are retained to all orders. The mathematical steps are outlined in Appendix.

The final expression for $G_{\omega,n}^{MF}(\hat{\sigma}_{ge}, \hat{\sigma}_{eg})$ is given by [45]

$$G_{\omega,n}^{MF}(\hat{\sigma}_{ge}, \hat{\sigma}_{eg}) = -\frac{1}{\omega_0 - \Delta - (\omega - n\Omega_0) - \sum_k \frac{|\tilde{\lambda}_k|^2}{\omega_k - (\omega - n\Omega_0)}}. \quad (22)$$

The same procedure can be used to calculate $G_\omega(\hat{\sigma}_{eg}, \hat{\sigma}_{ge})$ by using the mean-field approximation to write $G_t(\hat{\sigma}_{eg}, \hat{\sigma}_{ge}) \simeq e^{-[\Phi(0) - \Phi(t)]} G_t^{MF}(\hat{\sigma}_{eg}, \hat{\sigma}_{ge})$. The Fourier transform of $G_t^{MF}(\hat{\sigma}_{eg}, \hat{\sigma}_{ge})$, $G_\omega^{MF}(\hat{\sigma}_{eg}, \hat{\sigma}_{ge})$, can be obtained from the expression for $G_\omega^{MF}(\hat{\sigma}_{ge}, \hat{\sigma}_{eg})$ using the symmetry properties of the Green's functions. The absorption spectrum $\chi_a''(\omega)$ is defined as the imaginary part of the susceptibility Eq. (10), and by using $G_\omega(\hat{\sigma}_{ge}, \hat{\sigma}_{ge}) = G_\omega(\hat{\sigma}_{eg}, \hat{\sigma}_{eg}) = 0$ [45], we obtain

$$\begin{aligned} \chi_a''(\omega) &= \frac{N_d}{\epsilon_0 \hbar} |D_{ge}|^2 \text{Im} \left[\lim_{\epsilon \rightarrow 0} \sum_n L_n \frac{1}{\omega_0 - \Delta - (\omega - n\Omega_0) - \sum_k \frac{|\tilde{\lambda}_k|^2}{\omega_k - (\omega - n\Omega_0) - i\epsilon}} \right. \\ &\quad \left. + \lim_{\epsilon \rightarrow 0} \sum_n L_n \frac{1}{\omega_0 - \Delta + (\omega - n\Omega_0) - \sum_k \frac{|\tilde{\lambda}_k|^2}{\omega_k + (\omega - n\Omega_0) + i\epsilon}} \right]. \end{aligned} \quad (23)$$

Equation (23) is one of the central formal results of this article. The sideband structure is clearly seen in this expression. The self-energy terms $\sum_k \frac{|\tilde{\lambda}_k|^2}{\omega_k \pm (\omega - n\Omega_0) \pm i\epsilon}$ contain the details of the electromagnetic reservoir. We restrict our attention to those values of n and Ω_0 such that $\omega - n\Omega_0$ is close to the quantum dot transition frequency ω_0 . Terms with large values of n have vanishingly small spectral weights due to the rapid decrease of L_n with n , and the contribution of these sidebands to the line shape is negligible. Since ω_k is positive-definite, the second term in the expression for the optical susceptibility has a negligible imaginary part and can be dropped. In this analysis, phonon sidebands are centered at frequencies $\omega_0 + n\Omega_0$ and have widths determined by the parameter $|\tilde{\lambda}_k|^2 = |\langle \hat{C}_+ \rangle|^2 |\lambda_k|^2$. Clearly the coupling of the dot to the phonons in mean-field theory reduces the width of all spectral features by the Franck-Condon factor $\langle \hat{C}_+ \rangle \langle \hat{C}_- \rangle = e^{-\Phi(0)}$ [see Eq. (16)] when compared to the dot with no phonon coupling. The excited quantum dot is in a displaced lattice state compared to the phonon state when it is deexcited. The displaced states arise from a coherent superposition of phonons that surround the exciton and give rise to the polaron shift in its energy. The displacement of the many-body wave function grows with exciton-phonon coupling, g , and the number of thermally excited phonons. The greater the displacement of the phonon-dressed exciton, the weaker the effective exciton dipole transition rate.

This modification of the radiative decay rate by phonon dressing of the excited quantum dot is a distinguishing feature of our quantum-mechanical mean-field description, absent in other semiclassical treatments [47]. As we show in Sec. VC, the physical linewidth of the phonon sidebands is also heavily influenced by the lifetime of the phonons in the polaronic cloud. The damping of phonons (arising, for instance, from the breakup of phonons into lower energy phonons) limits the influence of the Franck-Condon effect and provides a more dominant channel for energy dissipation from the quantum dot excited state.

B. Polarization autocorrelation and excited-state lifetime

In this section, we derive general expressions for the polarization autocorrelation function and the lifetime of the excited state of a two-level system. In the absence of dot-photon coupling, $\hat{\sigma}_{ee}$ commutes with the rest of the Hamiltonian and there is no broadening of the zero-phonon line. The role of phonons is to induce pure dephasing without relaxation. In the presence of dot-photon coupling, there is line broadening due to radiative decay and the total rate of dephasing is due to both photon and phonon contributions. A simple two-level atom coupled to a free-space electromagnetic vacuum has a purely exponential decay. However, a two-level atom placed near a photonic bandgap exhibits non-Markovian radiative dynamics [8].

The polarization is defined as the temporal dipolar autocorrelation function:

$$P(t) = -i\Theta(t)\langle \hat{\sigma}_{ge}(t)\hat{\sigma}_{eg}(0) \rangle_H. \quad (24)$$

It describes the overlap between the initial system state (say the atom fully excited) and the state at a later time t . This captures the effects of dephasing due to the coupling of the two-level

atom to the electromagnetic modes and the phonon reservoir. Using the mean-field decomposition outlined previously, we rewrite Eq. (24) as

$$P_{MF}(t) \simeq -i\Theta(t)\langle \hat{\sigma}_{ge}(t)\hat{\sigma}_{eg}(0) \rangle_{H_{MF}} e^{-[\Phi(0) - \Phi(t)]}. \quad (25)$$

Since the polarization is defined only for $t > 0$, we relate the correlation function to the corresponding thermodynamic Green's function: $\langle \hat{\sigma}_{ge}(t)\hat{\sigma}_{eg}(0) \rangle_{H_{MF}} \simeq iG_t^{MF}(\hat{\sigma}_{ge}, \hat{\sigma}_{eg})$ for $\beta_s\omega_0 \gg 1$. Physically this follows from the fact that $\langle \hat{\sigma}_{eg}(0)\hat{\sigma}_{ge}(t) \rangle_{H_{MF}} \simeq 0$ for $\beta_s\omega_0 \gg 1$ since this term has a finite contribution only for the excited state. In thermal equilibrium and temperatures low compared to the quantum dot optical transition energy, the atom is primarily in the ground state. Therefore we have $P_{MF}(t) = \Theta(t)G_t^{MF}(\hat{\sigma}_{ge}, \hat{\sigma}_{eg})e^{-[\Phi(0) - \Phi(t)]}$. $G_t^{MF}(\hat{\sigma}_{ge}, \hat{\sigma}_{eg})$ can be evaluated by extending $G_\omega^{MF}(\hat{\sigma}_{ge}, \hat{\sigma}_{eg})$ on the whole complex plane and using the inverse-Laplace transform.

Until now we have focused solely on the equilibrium dynamics of the two-level atom interacting with a photon and a phonon reservoir. We now consider an important nonequilibrium problem of population dynamics of the two-level atom. The atom, at $t = 0$, is assumed to be in the excited state, and hence, its density matrix ceases to be of the canonical form $[\exp(-\beta H)/Z]$. In this section, we derive an expression for the lifetime of the excited state by studying the temporal evolution of $\langle \hat{\sigma}_{ee}(t) \rangle$ using the Heisenberg's equation of motion.

We now proceed with the Heisenberg equations of motion. Since $\hat{\sigma}_{ee}$ commutes with $\exp(-S)$, the equation of motion for the operator $\hat{\sigma}_{ee}$ can be written using either the Hamiltonian Eq. (1) or the polaron-transformed Hamiltonian Eq. (5). An approximate solution is obtained by solving the problem in the Born approximation in which the equation of motion for $\hat{\sigma}_{ee}(t)$ is considered to only second order in the dot-photon coupling. The dot-phonon coupling, on the other hand, is treated exactly to all orders and is subsequently approximated by thermal averages of the phonon displacement operators. The equation of motion for $\hat{\sigma}_{ee}(t)$ is easily shown to be given by

$$\begin{aligned} \frac{\partial \hat{\sigma}_{ee}(t)}{\partial t} = & - \left[\sum_k |\lambda_k|^2 \int_0^t dt' \hat{C}_+(t)\hat{\sigma}_{eg}(t)\hat{C}_-(t')\hat{\sigma}_{ge}(t') \right. \\ & \left. \times e^{-i\omega_k(t-t')} + \text{H.c.} \right] + \hat{N}(t), \end{aligned} \quad (26)$$

where $\hat{N}(t) = -i \sum_k \lambda_k e^{-i\omega_k t} \hat{C}_+(t)\hat{\sigma}_{eg}(t)\hat{a}_k(0) + \text{H.c.}$ and H.c. is the Hermitean conjugate. We now evaluate the quantum expectation value of this operator equation to calculate $\langle \hat{\sigma}_{ee}(t) \rangle = \text{Tr}(\rho_A \otimes \rho_{\text{phonon}} \otimes \langle \{0\} | \hat{\sigma}_{ee}(t) | \{0\} \rangle)$, where the atom is described by an arbitrary density matrix ρ_A , $\rho_{\text{phonon}} = \frac{e^{-\beta H_P}}{\text{Tr}(e^{-\beta H_P})}$ and $|\{0\}\rangle$ represents the photon vacuum. The phonon bath is assumed to be in thermal equilibrium at a temperature β .

We now need to evaluate $\langle \hat{C}_+(t)\hat{\sigma}_{eg}(t)\hat{C}_-(t')\hat{\sigma}_{ge}(t') \rangle$. In what follows, we perform the mean-field factorization $\langle \hat{C}_+(t)\hat{\sigma}_{eg}(t)\hat{C}_-(t')\hat{\sigma}_{ge}(t') \rangle \simeq \langle \hat{C}_+(t)\hat{C}_-(t') \rangle \langle \hat{\sigma}_{eg}(t)\hat{\sigma}_{ge}(t') \rangle$ and we provide a formal justification for relating the atomic polarization autocorrelation function to the atomic

population according to the relation $\langle \hat{\sigma}_{eg}(t) \hat{\sigma}_{ge}(t') \rangle \simeq e^{i\omega'_0(t-t')} \langle \hat{\sigma}_{eg}(t') \hat{\sigma}_{ge}(t') \rangle = e^{i\omega'_0(t-t')} \langle \hat{\sigma}_{ee}(t') \rangle$, where $\omega'_0 = \omega_0 - \Delta$ is the dressed atomic transition frequency.

We introduce the Liouvillian $\varepsilon = \varepsilon_0 + \varepsilon_p + \varepsilon_I$, where $\varepsilon_0 \hat{O}(t) = [\hat{O}(t), \tilde{H}_0]$, $\varepsilon_p \hat{O}(t) = [\hat{O}(t), H_p]$ and $\varepsilon_I \hat{O}(t) = [\hat{O}(t), \tilde{H}_I]$ for any general operator $\hat{O}(t)$ with $\tilde{H}_0 = (\omega_0 - \Delta) \hat{\sigma}_{ee} + \sum_k \omega_k \hat{a}_k^\dagger \hat{a}_k$, $\tilde{H}_I = \sum_k (\lambda_k \hat{C}_+ \hat{\sigma}_{eg} \hat{a}_k + \lambda_k^* \hat{a}_k^\dagger \hat{C}_- \hat{\sigma}_{ge})$, and $H_p = \sum_q \Omega_q \hat{c}_q^\dagger \hat{c}_q$. In terms of the Liouvillian, $\hat{\sigma}_{eg}(t) = e^{-i(\varepsilon_0 + \varepsilon_p + \varepsilon_I)(t-t')} \hat{\sigma}_{eg}(t')$. Since Eq. (26) is already second order in λ_k , the Born approximation implies that

$$\begin{aligned} \hat{\sigma}_{eg}(t) &\simeq e^{-i\varepsilon_p(t-t')} e^{-i\varepsilon_0(t-t')} \hat{\sigma}_{eg}(t') \\ &= e^{-i\varepsilon_0(t-t')} \hat{\sigma}_{eg}(t'), \end{aligned} \quad (27)$$

where we have used $\varepsilon_p \hat{\sigma}_{eg} = 0$. Evaluating Eq. (27), it is easy to see that $\hat{\sigma}_{eg}(t) \simeq e^{i(\omega_0 - \Delta)(t-t')} \hat{\sigma}_{eg}(t')$. Using the Born approximation, defined earlier, the right-hand side of Eq. (26) can be simplified to

$$\begin{aligned} \frac{\partial \langle \hat{\sigma}_{ee}(t) \rangle}{\partial t} &= - \left(\sum_k |\lambda_k|^2 \right. \\ &\quad \times \int_0^t dt' \langle \hat{C}_+(t) \hat{C}_-(t') \rangle \langle \hat{\sigma}_{eg}(t') \hat{\sigma}_{ge}(t') \rangle \\ &\quad \left. \times e^{i(\omega'_0 - \omega_k)(t-t')} + \text{H.c.} \right) + \hat{N}(t), \end{aligned} \quad (28)$$

where $\langle \hat{C}_+(t) \hat{C}_-(t') \rangle = \text{Tr}[\rho_{\text{phonon}} \hat{C}_+(t) \hat{C}_-(t')]$, $\langle \hat{\sigma}_{eg}(t) \hat{\sigma}_{ge}(t) \rangle = \text{Tr}[\rho_A \langle \{0\} | \hat{\sigma}_{ee}(t) | \{0\} \rangle]$, $\omega'_0 = \omega_0 - \Delta$, and $\hat{N}(t) = -i \sum_k \lambda_k e^{-i\omega_k t} \langle \hat{C}_+(t) \rangle \langle \hat{\sigma}_{eg}(t) \rangle \langle \hat{a}_k(0) \rangle + \text{H.c.}$

Using the thermal averages evaluated over the phonon reservoir $\langle \hat{C}_+(t) \hat{C}_-(t') \rangle$ given by Eq. (14) and the fact that the electromagnetic vacuum expectation values $\langle \hat{a}_k(0) \rangle = \langle \hat{a}_k^\dagger(0) \rangle = 0$, we rewrite Eq. (28) as

$$\frac{\partial \ell(t)}{\partial t} = - \int_0^t dt' e^{-(\Phi(0) - \Phi(t-t'))} G(t-t') \ell(t') - \text{c.c.} \quad (29)$$

where $\ell(t) = \langle \hat{\sigma}_{ee}(t) \rangle$, $G(t-t') = \sum_k |\lambda_k|^2 e^{i(\omega'_0 - \omega_k)(t-t')}$ and c.c. denotes complex conjugate. We solve this integro-differential equation for different photonic reservoirs in later sections.

IV. OPTICAL SUSCEPTIBILITY IN A PHOTONIC CRYSTAL

In this section, we calculate the optical susceptibility for a two-level atom inside a photonic crystal coupled to a phonon bath. Since the density of states changes rapidly in the vicinity of the photonic band edge, the Wigner-Weisskopf approximation is inadequate. In order to capture the non-Markovian nature of the atom-photon interaction, we must evaluate the self-energy more precisely [48,49].

A. Absorption spectra

We consider a simplified isotropic dispersion relation for the PBG material, obtained by expanding the photonic dispersion to leading order about the band edge wave vector k_0 . In the

effective mass approximation, it is given by

$$\omega_k = \omega_e + A(k - k_0)^2, \quad (30)$$

where ω_e is the band-edge frequency and A is a constant which depends on the photonic crystal parameters. For convenience of illustration, we choose $A = \frac{\omega_e}{k_0^2}$. A physical 3D photonic crystal is highly anisotropic and the isotropic dispersion model Eq. (30) is an oversimplification. On the other hand, the dispersion relation Eq. (30) can be realized in a 3D PBG material with a one-dimensional waveguide mode that has a cutoff inside the PBG [50,51].

For the structured electromagnetic vacuum defined by Eq. (30), the self-energy term in Eq. (23) can be easily evaluated [8,38] to yield the (non-Lorentzian) absorption line:

$$\begin{aligned} \chi_a(\omega) &= - \frac{N_d}{\epsilon_0 \hbar} |D_{ge}|^2 \left[\sum_n L_n \right. \\ &\quad \left. \times \frac{1}{(\omega - n\Omega_0) - \omega_0 + \Delta + e^{-\Phi(0)} \frac{iC}{\sqrt{(\omega - n\Omega_0) - \omega_e}}} \right] \end{aligned} \quad (31)$$

with $C = \frac{\omega_0^2 |D_{ge}|^2}{12\pi \epsilon_0 \hbar} \frac{k_0^3}{\omega_e^{3/2}}$, $L_n = e^{-g(2N+1)} e^{n\Omega_0 \beta/2} I_n [2g\sqrt{N(N+1)}]$, and we have absorbed the Lamb shift into the resonant frequency of the quantum dot. In the limit of vanishing coupling to phonons, the expression for susceptibility reduces to

$$\chi_a(\omega) = - \frac{N_d}{\epsilon_0 \hbar} |D_{ge}|^2 \frac{1}{\omega - \omega_0 + \frac{iC}{\sqrt{\omega - \omega_e}}}. \quad (32)$$

Clearly, this susceptibility has no imaginary part for $\omega < \omega_e$ and there is no absorption inside the PBG. However, when the coupling to phonons is included, the atom can absorb at frequencies inside the band gap by phonon-assisted processes. For example, for $\omega_0 < \omega_e$ and $\Omega_0 > \omega_e - \omega_0$, the $n = 1$ term describes the absorption of a photon whose energy is outside the gap assisted by an emission of a phonon into the thermal reservoir. The contribution of higher order phonon processes becomes progressively smaller due to smaller spectral weights attached to them, but the probability of a phonon-mediated process increases with rise in temperature.

In Fig. 1, we plot the absorption spectra of a quantum dot in the structured reservoir of a photonic crystal. The quantum dot transition frequency is 1 eV, and the optical phonon frequency is 0.01 eV. Temperature is measured in units of eV⁻¹. Absorption is seen for frequencies inside the photonic band gap at strong dot-phonon coupling strengths and high temperatures. At low cryogenic temperatures and weak dot-phonon coupling, the absorption spectrum is dominated by the zero-phonon line.

B. Polarization of the two-level atom in a photonic crystal

In this section, we consider the effect of phonons on the polarization (coherence) of the two-level system inside a photonic crystal. For an excited atom whose resonant frequency is near the band edge, the atom is dressed by its own localized radiation field. This leads to Rabi splitting of the excited state into an Autler-Townes doublet [8]. If the dressing is strong enough, the lower frequency component of the doublet is

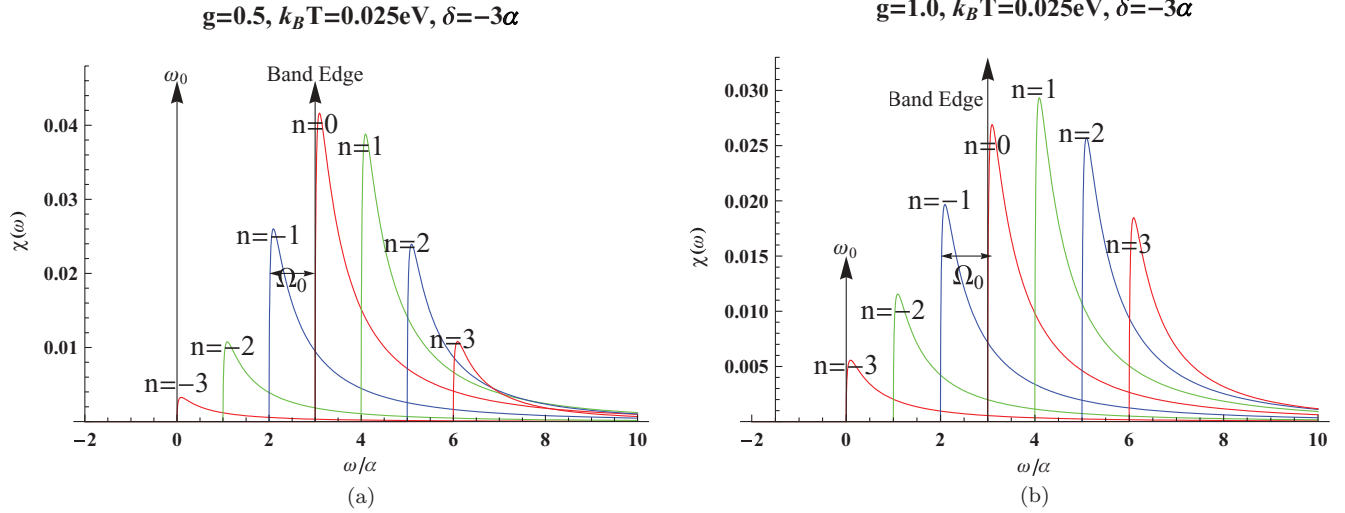


FIG. 1. (Color online) Plots of absorption spectra $\chi(\omega)$ (in arbitrary units) defined in Eq. (31) of the quantum dot slightly detuned from a photonic band edge in a photonic crystal. In the absence of direct nonradiative decay and phonon damping, the radiative line shapes are modified by the non-Markovian interaction with the photonic band edge. The quantum dot transition is assumed to be 1 eV, and the optical phonon frequency is .01 eV. Temperature is chosen 1/40 eV for all the plots. The frequency scale is $\alpha = C^{2/3}$, where $C = \frac{\omega_0^2 |D_{ge}|^2}{12\pi\epsilon_0\hbar} \frac{k_0^3}{\omega_e^3/2}$. The sidebands (separated by Ω_0 in frequency) have been shifted for comparison in the same plot. The band edge and the resonant frequency of the atom are shown with respect to the zero-phonon line. The dot-phonon coupling $g = \sum \frac{y_j^2}{\Omega_j^2}$ is 0.5 in (a) and $g = 1.0$ in (b). The detuning $\delta = -3\alpha$ (inside PBG). The effect of phonon sidebands is clearly seen at room temperatures ($k_B T = \frac{1}{40}$ eV). Absorption inside the band gap is noticeable due to enhanced phonon-mediated absorption due to strong dot-phonon coupling and an increase in temperature of the phonon bath. Phonon-mediated absorption also increases with the dot-phonon coupling strength. For low temperatures ($k_B T \approx 10^{-3}$ eV), we expect no phonon-assisted absorption. The spectral weight in the sidebands is also smaller at low temperatures. In the absence of phonon damping, the width of all the peaks is purely radiative in nature.

pushed inside the photonic band gap and this component is immune from spontaneous radiative decay. This photon-atom bound state results in a nonzero steady-state population and finite coherence for large times. In the model Hamiltonian of Eq. (1) and our subsequent mean-field theory, the role of phonons is to dephase the optical dipole of the quantum dot and to displace the excited state wave function from that of the ground state. This leads to diminished polarization and coherence but to an enhanced excited state population for the photon-atom bound state. In this model, the lifetime of the photon-atom bound state is limited by damping of the phonons themselves due to anharmonic or dissipative processes. The important role of the phonon lifetime in modifying the photon-atom bound state is discussed in Sec. V C.

We now study the temporal evolution of the polarization of an initially excited quantum dot coupled to the structured electromagnetic reservoir of the photonic crystal and a bath of thermalized optical phonons. The coherence of the two-level atom coupled to phonons is $|P_{MF}(t)|$ as defined by Eq. (25). It is easily shown to be given by

$$P_{MF}(t) = -i\Theta(t) \sum_n L_n e^{-i(n\Omega_0 + \omega_e)t} \times \left[2a_1 x_1 e^{\alpha x_1^2 t} + a_2 (x_2 + y_2) e^{\alpha x_2^2 t} - \sum_{j=1}^3 a_j y_j \text{Erfc}(\sqrt{\alpha x_j^2 t}) e^{\alpha x_j^2 t} \right]. \quad (33)$$

The definition of constants a_i 's and x_i 's and the detailed derivation of Eq. (33) can be found in [8]. In the absence of any coupling to phonons ($L_0 = 1$ and $L_n = 0$ for all $n \neq 0$), it has been shown [8] that for ω_0 near the band edge, strong interaction between the atom and its localized radiation splits the atomic level into dressed states. These dressed states are formed at frequencies $\omega_e - \alpha \text{Im}(x_1^2)$ and $\omega_e - \alpha \text{Im}(x_2^2)$. The first dressed state is pushed inside the gap, and this bound state leads to the fractionalized steady-state atomic population in the excited state. However, in the presence of phonon coupling, we see using Eq. (33) that there exists an infinite number of dressed states formed at frequencies $\omega_e - n\Omega_0 - \alpha \text{Im}(x_1^2)$ and $\omega_e - n\Omega_0 - \alpha \text{Im}(x_2^2)$. The relative spectral weights of these dressed states are determined by L_n . For low β and large g , the spectral weight is distributed over a large number of phonon sidebands. However for low temperatures (cryogenic temperatures, high β) and $g \ll 1$, the spectral weight is contained in a few sidebands about the zero-phonon line. The short time \sim ps temporal evolution of polarization of the two-level atom is determined by the interference of these sidebands. However, undamped optical phonons do not lead to complete dephasing at long time scales. Moreover, the coupling of the two-level system to the phonon bath results in a Franck-Condon shift that reduces the optical dipole-moment resulting in slower electromagnetic dephasing. The ultimate cause of decoherence and decay of the photon-atom bound state occurs from damping (finite lifetime) of the phonons themselves or from other nonradiative decay channels (see Sec. V).

C. Population dynamics of the fractionalized steady state

We now calculate the residual population on the fractionalized steady state. We start from Eq. (29), which we solve using the method of Laplace transforms. The Laplace transform of $\ell(t)$ is given by

$$\tilde{\ell}(s) = \frac{\ell(0)}{s + \sum_n L_n \tilde{Z}(s - in\Omega_0) + \sum_n L_n \tilde{Z}^*(s - in\Omega_0)}, \quad (34)$$

where the self-energy $\tilde{Z}(s)$ is easily evaluated [14,38] for the isotropic dispersion relation Eq. (30) and is given by

$$\tilde{Z}(s - in\Omega_0) = \frac{\alpha^{\frac{3}{2}} e^{-\frac{i\pi}{4}}}{\sqrt{s - i\delta + in\Omega_0}}, \quad (35)$$

where $\alpha^{\frac{3}{2}} = \frac{\omega_0^{\frac{7}{2}} |D_{ge}|^2}{6\pi\epsilon_0\hbar c^3}$. The resulting inverse-Laplace transform cannot be evaluated analytically, and the inversion is done numerically. At zero temperature, $L_n = 0$ for $n < 0$ ("hot" sidebands inactive) since there are no phonons available to absorb from the thermal phonon reservoir. Only the cold bands ($n > 0$), involving phonon emission contribute to the spectrum. At finite temperatures, all sidebands are active, and the weight of L_n 's, for $n < 0$, increases with temperature. With increasing temperatures, there is a marginal shift in the spectral weight to the $n < 0$ sidebands.

The dressing of the photon-atom bound state by the phonons leads to (i) a shift of the spectral weight further inside the photonic band gap due to the polaron shift, (ii) a reduction of the effective transition dipole moment due to dephasing, and (iii) a diminished overlap between the excited state many-body (atom + phonon cloud) wave function from the ground state. In the absence of phonon damping, this leads to the peculiar result that optical phonons suppress radiative decay. In the next section, we consider additional physical effects that need to be included for a realistic picture of quantum dot phonon interactions.

V. ROLE OF ACOUSTIC PHONONS, NONRADIATIVE RELAXATION, AND PHONON LIFETIME

In the previous section, we studied phonon-mediated relaxation of a quantum dot using a purely optical phonon bath and photons. In this section, we reconsider polarization and population decay dynamics of the quantum dot with coupling to acoustic phonons. We also include a purely nonradiative decay channel in our model Hamiltonian. Finally we consider anharmonic phonon processes described by a phenomenological damping parameter. These processes enable complete decay of the photon-atom bound state.

A. Undamped acoustic phonons

The optical phonon model used in the previous sections led to well-separated phonon sidebands. Interference between these sidebands gives rise to oscillations in the polarization at optical phonon timescales. However, the polarization of a photon-atom bound state does not decay to zero at long times. For coupling to a continuum of acoustic phonons, the distinct sidebands likewise merge into a continuum.

Quantum interference within this continuum of modes leads to polarization decay to a new steady state without any subsequent revivals.

For acoustic phonons, we adopt a model used in earlier literature [17,18] to describe GaAs-based quantum dots. Assuming a spherical dot model with acoustic deformation potential interactions, the dot-phonon coupling is

$$\eta_q = \left(\frac{\hbar q}{2\rho c_l V} \right)^{\frac{1}{2}} (D_e - D_h) \exp\left(-\frac{q^2 L^2}{4}\right), \quad (36)$$

where $\rho = 5379 \text{ kg m}^{-3}$ is the mass density of GaAs, $c_l = 5110 \text{ m/s}$ is the longitudinal sound velocity, $D_e = -14.6 \text{ eV}$ and $D_h = -4.8 \text{ eV}$ are the deformation potentials for electrons and holes, and $L = 5 \text{ nm}$ is the electronic localization length in the quantum dot. The exponential in Eq. (36) introduces an effective cutoff in q ; hence, an explicit cutoff at the Debye wave vectors is not required. Typical material parameters for GaAs with a quantum dot electronic localization length $L = 5 \text{ nm}$ lead to characteristic time and energy (temperature) scales of $\tau = L/c_l \simeq 1 \text{ ps}$ and $\hbar/\tau \simeq 0.7 \text{ meV}$ (7.8 K), respectively. For small q 's, an effective linear dispersion relation $\Omega_q = c_l q$ is assumed and Eq. (15) for $\Phi(t)$ is now given by

$$\Phi(t) = \alpha_p \int_0^\infty dx x \exp\left(-\frac{x^2}{2}\right) \left[i \sin(x\bar{t}) + \cos(x\bar{t}) \coth\left(\frac{\hbar\beta x}{2\tau}\right) \right], \quad (37)$$

where $\bar{t} = \frac{t}{\tau}$ and the dimensionless dot-phonon coupling (Huang-Rhys factor) α_p is defined as

$$\alpha_p = \frac{(D_e - D_h)^2}{4\pi^2 \hbar \rho c_l^3 L^2} \simeq 0.033. \quad (38)$$

An analytic expression for $\Phi(t)$ can be derived by approximating $\coth\left(\frac{\hbar\beta x}{2\tau}\right) \simeq \frac{2\tau}{\hbar\beta x}$ which is certainly valid for $\frac{\hbar\beta x}{2\tau} \ll 1$ ($T \gg 7.8 \text{ K}$). The integrals are straightforward to perform analytically, and we obtain:

$$\Phi(t) = \alpha_p (\bar{t}) e^{-\frac{\bar{t}^2}{2}}, \quad (39)$$

where $\alpha_p(\bar{t}) = \alpha_p^{(1)} + i\bar{t}\alpha_p^{(2)}$ and $\alpha_p^{(1)} = \frac{\sqrt{2\pi}\alpha_p\tau}{\hbar\beta}$ and $\alpha_p^{(2)} = \sqrt{\frac{\pi}{2}}\alpha_p$. The spectral weight of the zero-phonon line, $e^{-\Phi(0)}$, is now given by $e^{-\alpha_p^{(1)}}$.

We now consider the population decay dynamics Eq. (29) in the presence of an acoustic phonon reservoir. Unlike the case of optical phonons, a straightforward expansion in terms of the phonon sidebands cannot be made. Using Eq. (39) in Eq. (29) for $\ell(t)$, we obtain

$$\frac{\partial \ell(t)}{\partial t} \simeq -e^{-\Phi(0)} \sum_k |\lambda_k|^2 \int_0^t dt' e^{\alpha_p(\frac{t-t'}{\tau})} e^{-\frac{(t-t')^2}{2}} \times \ell(t') e^{i(\omega_0 - \omega_k)(t-t')} + \text{c.c.}, \quad (40)$$

where $\alpha_p(\frac{t-t'}{\tau}) = \alpha_p^{(1)} + i\frac{t-t'}{\tau}\alpha_p^{(2)}$. A straightforward scaling analysis shows that for $t \ll \alpha^{-1}$, $\frac{\partial \ell(t)}{\partial t} \simeq 0$. The right-hand side of Eq. (40) is nonzero only for $t \geq \alpha^{-1}$ when population decay kicks in due to radiative processes which happen on timescales of α^{-1} . This is due to the fact that the role of phonons is

confined to pure dephasing [as modeled using the Independent-Boson model for the dot-phonon dynamics in Eq. (1)] wherein phonons do not cause any population decay [since $\hat{\sigma}_{ee}$ commutes with the phonon part of the interaction Hamiltonian in Eq. (1)] but are only associated with polarization decay.

The radiative memory kernel $\Sigma(t-t') \equiv \sum_k |\lambda_k|^2 e^{i(\omega'_0 - \omega_k)(t-t')}$ describes non-Markovian effects in the vicinity of a photonic band edge. When the radiative transition is detuned by a small amount, δ , from a $1-D$ band edge singularity in the electromagnetic density of states, this memory kernel decays [14] as a power law $\Sigma(t-t') \simeq \frac{\alpha \frac{3}{2} e^{-\frac{i\pi}{4}} e^{i\delta(t-t')}}{\sqrt{t-t'}}$. Phonon dephasing effects tend to suppress these memory effects. The more phonons that participate in the decay process, the more rapidly memory is lost.

The primary effect of undamped acoustic phonons in our model is a very rapid decay of polarization at picosecond timescales followed by radiative decay at long timescale but with a reduction in strength of the effective radiative coupling $|\lambda_k|^2$ due to the Franck-Condon shift of the excited state wave function. In a PBG material, the excited-state population in the photon-atom bound state is enhanced. Despite the continuum of acoustic phonon modes, the model Hamiltonian does not allow for decay of the system to its ground state by pure phonon effects. This picture is valid at very low temperatures. In an ordinary vacuum, this corresponds to the situation where the dynamics of quantum dots and their polarization decay is “radiatively limited” [29,32,33]. In a PBG material, where radiative processes can be suspended on timescales much longer than in ordinary vacuum, it is important to consider additional channels for phonon-mediated decay of the photon-atom bound state. This is the subject for the next two subsections.

B. Addition of purely nonradiative decay channel

Our model Hamiltonian Eq. (1) recaptures certain features of multiple-phonon-assisted radiative transitions. In this picture, the quantum dot excited state is dressed by various numbers of phonons, leading to a series of sidebands with energies determined by the number and energy of phonons involved. However, transitions from these dressed states to the quantum dot ground state are purely radiative in nature. The spectral width of these sidebands is determined by the optical density of states at the sideband transition frequency and the modified optical transition matrix element. The optical transition dipole, in this simple model, is diminished due to phonon dephasing effects and the Franck-Condon displacement of the dressed excited states from the ground state. This leads to an artificially small linewidth to the phonon sidebands. In a more realistic picture, we must incorporate phonon-mediated decay mechanisms in addition to the phonon-mediated dressing of the excited state. As we will show, these additional decay channels limit the extent to which the optical dipole transition can be suppressed by the Franck-Condon effect and provide a more realistic picture of the spectral linewidths of the phonon sidebands.

In this subsection, we introduce pure nonradiative decay due to phonons through an additional term in the interaction

Hamiltonian:

$$H_{\text{decay}} = \sum_p (\zeta_p \hat{\sigma}_{eg} \hat{d}_p + \zeta_p^* \hat{d}_p^\dagger \hat{\sigma}_{ge}), \quad (41)$$

where $\hat{d}_p^\dagger(\hat{d}_p)$ is the creation (annihilation) operator for the decay phonon with wave number p . We assume that these decay phonons form a continuum with a smooth and featureless (vibrational) density of states. The operator \hat{d}_p^\dagger could, for instance, correspond to the simultaneous creation of many phonons of the type described earlier with energies $\{\hbar\Omega_{k_i}\}$ such that $p = \sum_i k_i$ and $\hbar\omega_0 \simeq \sum_i \hbar\Omega_{k_i}$. Rather than solving the full Hamiltonian, we capture the role of this decay term by introducing a phenomenological decay rate, γ_{nonrad} , for the excited state amplitude. In the limiting case of $H_I = 0$ [see Eq. (1b)], this corresponds to the replacement $\omega_0 \rightarrow \omega_0 - i\gamma_{\text{nonrad}}$ and the decay of the two-level atom correlation function is given by $-i\Theta(t)\langle\hat{\sigma}_{ge}(t)\hat{\sigma}_{eg}(0)\rangle = -i\Theta(t)e^{-i\omega_0 t} \exp(-\gamma_{\text{nonrad}}t)$.

We start by considering the effect of H_{decay} on the “Independent-Boson part” of the Hamiltonian H in Eq. (1). The modified Independent-Boson Hamiltonian becomes

$$H_0 = \hbar\omega_0 \hat{\sigma}_{ee} + \sum_q \hbar\Omega_q \hat{c}_q^\dagger \hat{c}_q + \sum_p \hbar\xi_p \hat{d}_p^\dagger \hat{d}_p, \quad (42a)$$

$$H_I^{\text{decay}} = \hat{\sigma}_{ee} \sum_q \eta_q (\hat{c}_q + \hat{c}_q^\dagger) + H_{\text{decay}}. \quad (42b)$$

The correlation function $g(t) = -i\Theta(t)\langle\hat{\sigma}_{ge}(t)\hat{\sigma}_{eg}(0)\rangle$ for the unperturbed Independent-Boson Hamiltonian is well known [17,40]. Using the linked-cluster theorem [40], the correlation function can be written as $g(t) = g^0(t)e^{W(t)}$. Here $g^0(t) = -i\Theta(t)e^{-i\omega_0 t}$ is the two-level atom propagator in the absence of the dot-phonon interaction and $W(t)$ is given by [40]

$$W(t) = -e^{i\omega_0 t} \int_0^t dt_1 \int_0^{t_1} dt_2 D(t_1 - t_2) \times g^0(t - t_1)g^0(t_1 - t_2)g^0(t_2) \quad (43)$$

and $D(t_1 - t_2)$ is the phonon correlation function [40] defined as

$$iD(t_1 - t_2) = \sum_q \eta_q^2 [(N_q + 1)e^{-i\Omega_q|t_1 - t_2|} + N_q e^{i\Omega_q|t_1 - t_2|}]. \quad (44)$$

It is now straightforward to show [52] that $g(t) = -i\Theta(t)e^{-i(\omega_0 - \Delta)t} e^{-[\Phi(0) - \Phi(t)]}$. This is the well-known result [40] for the Independent-Boson model with $\Phi(t)$ and Δ defined in Eqs. (15) and (6), respectively.

We now consider the effect of the decay term, H_{decay} , on the correlation function of the Independent-Boson Hamiltonian. This decay term interferes with the pure phonon dephasing process. If the timescale of the decay-phonon processes is substantially faster than the pure dephasing phonons, the atom will undergo nonradiative decay even before it can transfer energy and emit or absorb pure dephasing phonons. If the timescales of these two phonon processes are comparable, the spectral structure of the phonon sidebands due to pure dephasing phonons should be modified by the nonradiative decay processes. The contribution of this decay term to the Independent-Boson correlation function can be included

in the lowest order by the ansatz [53]:

$$D(t_1 - t_2) \rightarrow D(t_1 - t_2)e^{-\gamma_{\text{nonrad}}|t_1 - t_2|}. \quad (45)$$

A microscopic derivation of this replacement follows from the interaction Hamiltonian Eq. (41). Our ansatz corresponds to the leading correction to the irreducible self-energy of the temporal atomic dipole propagator, arising from the additional interaction Eq. (41). The decay term acts only during the times when the dot interacts with the purely dephasing phonons and leads to the renormalization of the dot-pure dephasing phonon coupling due to direct nonradiative processes. This simultaneous interaction of the nonradiative decay processes and purely dephasing processes results in broadening of the phonon sidebands. A microscopic expression for γ_{nonrad} can be obtained from H_{decay} . To the lowest order in the dot-nonradiative decay coupling, we obtain $\gamma_{\text{nonrad}} = \pi \sum_p (n_p + \frac{1}{2}) |\zeta_p|^2 \delta(\omega - \xi_p)$, where $n_p = \frac{1}{e^{\beta \xi_p} - 1}$. The excited state probability then decays as $e^{-2\gamma_{\text{nonrad}} t}$. Assuming a smooth density of states in the vicinity of ω_0 , the sum can be converted into an integral and evaluated. For $\beta \xi_p \ll 1$, it is easy to see that γ_{nonrad} is linear in T . Therefore, in this simple model, we find that the nonradiative decay rate increases linearly with temperature (in the high-temperature limit $\beta \xi_p \ll 1$).

Using Eq. (45) in Eq. (43) and evaluating the time integrals [35], $W(t)$ can be expressed in terms of the modified phonon correlation function $\tilde{\Phi}(t)$ as

$$W(t) = -t\tilde{\Phi}'(0) - [\tilde{\Phi}(0) - \tilde{\Phi}(t)], \quad (46a)$$

$$\tilde{\Phi}(t) = \sum_q \eta_q^2 \left[\frac{N_q}{(\Omega_q + i\gamma_{\text{nonrad}})^2} e^{i(\Omega_q - \gamma_{\text{nonrad}})t} + \frac{N_q + 1}{(\Omega_q - i\gamma_{\text{nonrad}})^2} e^{-i(\Omega_q - \gamma_{\text{nonrad}})t} \right]. \quad (46b)$$

It is convenient to write $\tilde{\Phi}(t) = \tilde{\Phi}_1(t) + i\tilde{\Phi}_2(t)$. Also note $\tilde{\Phi}(0)$ can be decomposed as $\tilde{\Phi}(0) = \tilde{\Phi}_1(0) + i\tilde{\Phi}_2(0)$, where $e^{-\tilde{\Phi}_1(0)}$ is the spectral weight of the zero-phonon line [35] and $\tilde{\Phi}_2(0)$ is a phase. Also $\tilde{\Phi}'(0) = \frac{d\tilde{\Phi}(t)}{dt}|_{t=0} = \tilde{\gamma}_{\text{nonrad}} - i\tilde{\Delta}$, where $\tilde{\gamma}_{\text{nonrad}}$ is an additional decay term contributing to polarization decay due to modified pure dephasing caused by H_{decay} and $\tilde{\Delta}$ is the new polaron shift. They are given by

$$\tilde{\gamma}_{\text{nonrad}} = \sum_q \frac{\eta_q^2 \gamma_{\text{nonrad}}}{\Omega_q^2 + \gamma_{\text{nonrad}}^2} (1 + 2N_q), \quad (47)$$

$$\tilde{\Delta} = \sum_q \eta_q^2 \frac{\Omega_q}{\Omega_q^2 + \gamma_{\text{nonrad}}^2}.$$

We now study an analytical and instructive example of the modification of the phonon correlation function due to nonradiative decay γ_{nonrad} using the acoustic phonon model described in the previous subsection [Eqs. (36)–(38)]. The modified function $W(t)$ Eq. (43) now takes the form:

$$W(t) = \alpha_p \int_0^t dt_1 \int_0^{t_1} dt_2 \int_0^\infty dx x^3 \exp\left(-\frac{x^2}{2}\right) \times \left[i \sin(x\bar{t}_{12}) - \cos(x\bar{t}_{12}) \coth\left(\frac{\hbar\beta x}{2\tau}\right) \right] e^{-\bar{\gamma}_{nr}\bar{t}_{12}}, \quad (48)$$

where $\bar{\gamma}_{nr} \equiv \gamma_{\text{nonrad}}\tau$ and $\bar{t}_{12} \equiv (t_1 - t_2)/\tau$. We now approximate $\coth\left(\frac{\hbar\beta x}{2\tau}\right) = \frac{2\tau}{\hbar\beta x}$ as in Eq. (39). The modified phonon correlation function can now be obtained using Eq. (46a) following a straightforward evaluation of Eq. (48):

$$\tilde{\Phi}_1(t) = \alpha_p^{(1)} e^{-\frac{\bar{t}}{2}(2\bar{\gamma}_{nr} + \bar{t})} \left[(1 + \bar{\gamma}_{nr}^2) + \sqrt{\frac{\pi}{2}} \bar{\gamma}_{nr} e^{\frac{1}{2}(\bar{\gamma}_{nr} + \bar{t})^2} \times (2 + \bar{\gamma}_{nr}^2 + 2\bar{\gamma}_{nr}\bar{t}) \text{Erf}\left(\frac{\bar{\gamma}_{nr} + \bar{t}}{\sqrt{2}}\right) \right], \quad (49a)$$

$$\tilde{\Phi}_2(t) = -\alpha_p^{(2)} e^{-\frac{\bar{t}}{2}(2\bar{\gamma}_{nr} + \bar{t})} \left[(2\bar{\gamma}_{nr} + \bar{\gamma}_{nr}^3 - \bar{t}) + \bar{\gamma}_{nr}^2 e^{\frac{1}{2}(\bar{\gamma}_{nr} + \bar{t})^2} \times \sqrt{\frac{\pi}{2}} (3 + \bar{\gamma}_{nr}^2 + \bar{\gamma}_{nr}\bar{t}) \text{Erf}\left(\frac{\bar{\gamma}_{nr} + \bar{t}}{\sqrt{2}}\right) \right]. \quad (49b)$$

The zero-phonon line intensity ($e^{-\tilde{\Phi}_1(0)}$) which is determined by $\tilde{\Phi}_1(0)$ and the phase $\tilde{\Phi}_2(0)$ are easily extracted from the preceding discussion. It is instructive to consider the situation in which direct nonradiative decay is weak perturbation compared to the dot-acoustic phonon coupling ($\bar{\gamma}_{nr} \equiv \gamma_{\text{nonrad}}\tau \ll 1$). In this case, we make a power-series expansion in $\bar{\gamma}_{nr}$ to obtain

$$\tilde{\Phi}_1(0) = \alpha_p^{(1)} [1 + 3\bar{\gamma}_{nr}^2 + O(\bar{\gamma}_{nr}^4)], \quad (50a)$$

$$\tilde{\Phi}_2(0) = -2\alpha_p^{(2)} [\bar{\gamma}_{nr} + 2\bar{\gamma}_{nr}^3 + O(\bar{\gamma}_{nr}^5)]. \quad (50b)$$

Note that the spectral weight of the zero-phonon line $e^{-\tilde{\Phi}_1(0)}$ decreases with increasing nonradiative decay. The decay term in the modified phonon correlation function, $\tilde{\gamma}_{\text{nonrad}}$ (which causes exponential decay at long times $t \gg \tau$), and the modified polaron shift $\tilde{\Delta}$ are now obtained using $\tilde{\Phi}_1(0)$ and $\tilde{\Phi}_2(0)$, respectively:

$$\tilde{\gamma}_{\text{nonrad}} = \alpha_p^{(1)} \gamma_{\text{nonrad}} \left[1 + \sqrt{\frac{\pi}{2}} \bar{\gamma}_{nr} e^{\frac{\bar{\gamma}_{nr}^2}{2}} \text{Erf}\left(\frac{\bar{\gamma}_{nr}}{\sqrt{2}}\right) \right], \quad (51a)$$

$$\tilde{\Delta}\tau = \alpha_p^{(2)} \left[(1 - \bar{\gamma}_{nr}^2) - \sqrt{\frac{\pi}{2}} \bar{\gamma}_{nr}^3 e^{\frac{\bar{\gamma}_{nr}^2}{2}} \text{Erf}\left(\frac{\bar{\gamma}_{nr}}{\sqrt{2}}\right) \right]. \quad (51b)$$

A Taylor expansion of $\tilde{\gamma}_{\text{nonrad}}$ and $\tilde{\Delta}$ lead to

$$\tilde{\gamma}_{\text{nonrad}}\tau = \alpha_p^{(1)} \bar{\gamma}_{nr} [1 + \bar{\gamma}_{nr}^3 + O(\bar{\gamma}_{nr}^5)], \quad (52a)$$

$$\tilde{\Delta}\tau = \alpha_p^{(2)} [1 - \bar{\gamma}_{nr}^2 + O(\bar{\gamma}_{nr}^4)]. \quad (52b)$$

Note that $\tilde{\gamma}_{\text{nonrad}} \rightarrow 0$ as $\gamma_{\text{nonrad}} \rightarrow 0$ as one would expect. Moreover, the modified polaron shift $\tilde{\Delta}$ decreases with increasing γ_{nonrad} reflecting the fact that polaronic effects are suppressed by direct nonradiative effects.

The short-time phonon dynamics $t \ll \tau$ of $e^{-[\tilde{\Phi}(0) - \tilde{\Phi}(t) + t\tilde{\Phi}'(0)]}$ can be obtained by expanding $\tilde{\Phi}(0) - \tilde{\Phi}(t) + t\tilde{\Phi}'(0)$ as a power series in \bar{t} which is found to be given by

$$\tilde{\Phi}(0) - \tilde{\Phi}(t) + t\tilde{\Phi}'(0) = \frac{\alpha_p^{(1)}}{2} \bar{t}^2 + O(\bar{t}^3). \quad (53)$$

Neglecting terms \bar{t}^3 and higher, we find that the absorption spectrum which is the Fourier transform of the dipolar autocorrelation function is

$$\chi''(\omega) = \frac{1}{\sqrt{2\pi D}} e^{-\frac{(\omega - \omega_0)^2}{2D^2}}, \quad (54)$$

where ω_0 is the bare quantum dot transition frequency and $D^2 = \frac{\alpha_p^{(1)}}{\tau^2}$ is the width of the Gaussian spectrum. Note that $D \propto \sqrt{T}$ and the width of the sidebands increases with temperature.

The long-time phonon dynamics ($t \gg \tau$) is easy to obtain by making an asymptotic expansion of $\tilde{\Phi}(t) = \tilde{\Phi}_1(t) + i\tilde{\Phi}_2(t)$ in Eq. (49) as follows:

$$\begin{aligned} \tilde{\Phi}_1(t) = \alpha_p^{(1)} \left\{ e^{\frac{\tilde{\gamma}_{nr}^2}{2}} \sqrt{\frac{\pi}{2}} [\bar{\gamma}_{nr}^2 \bar{t} + \bar{\gamma}_{nr} (2 + \bar{\gamma}_{nr}^2)] \right. \\ \left. + e^{-\frac{i}{2}(2\bar{\gamma}_{nr}^2 + \bar{t})} \left[1 - \frac{2\bar{\gamma}_{nr}}{\bar{t}} + \frac{3\bar{\gamma}_{nr}^2}{\bar{t}^2} + O\left(\frac{1}{\bar{t}^3}\right) \right] \right\}, \end{aligned} \quad (55a)$$

$$\begin{aligned} \tilde{\Phi}_2(t) = -\alpha_p^{(2)} \left\{ \sqrt{\frac{\pi}{2}} e^{\frac{\tilde{\gamma}_{nr}^2}{2}} [\bar{\gamma}_{nr}^3 \bar{t} + \bar{\gamma}_{nr}^2 (3 + \bar{\gamma}_{nr}^2)] \right. \\ \left. - e^{-\frac{i}{2}(2\bar{\gamma}_{nr} + \bar{t})} \left[\bar{t} - 2\bar{\gamma}_{nr} + \frac{3\bar{\gamma}_{nr}^2}{\bar{t}} + O\left(\frac{1}{\bar{t}^2}\right) \right] \right\}. \end{aligned} \quad (55b)$$

For large \bar{t} , we consider Eq. (55) to leading order and obtain

$$\tilde{\Phi}_1(t) \simeq \alpha_p^{(1)} e^{\frac{\tilde{\gamma}_{nr}^2}{2}} \sqrt{\frac{\pi}{2}} [\bar{\gamma}_{nr}^2 \bar{t} + \bar{\gamma}_{nr} (2 + \bar{\gamma}_{nr}^2)], \quad (56a)$$

$$\tilde{\Phi}_2(t) \simeq -\alpha_p^{(2)} \sqrt{\frac{\pi}{2}} e^{\frac{\tilde{\gamma}_{nr}^2}{2}} [\bar{\gamma}_{nr}^3 \bar{t} + \bar{\gamma}_{nr}^2 (3 + \bar{\gamma}_{nr}^2)]. \quad (56b)$$

For simplicity, denote $\tilde{\Phi}_1(t) = \tilde{\Phi}_1^{(1)}(0) + \tilde{\Phi}_1^{(2)}\bar{t}$ in Eq. (56). Similarly we denote $\tilde{\Phi}_2(t) = \tilde{\Phi}_2^{(1)}(0) + \tilde{\Phi}_2^{(2)}\bar{t}$. The dipole autocorrelation function now has the following asymptotic form for $t \gg \tau$:

$$\begin{aligned} e^{-i(\omega_0 - \tilde{\Delta})t} e^{-[\tilde{\Phi}(0) - \tilde{\Phi}(t)] - \tilde{\gamma}_{\text{nonrad}} t} \\ \simeq e^{-i(\omega_0 - \tilde{\Delta})t} e^{-[\tilde{\Phi}_1^{(1)}(0) - \tilde{\Phi}_1^{(1)}(0)]} e^{-i[\tilde{\Phi}_2^{(1)}(0) - \tilde{\Phi}_2^{(1)}(0)]} \\ \times e^{-[\tilde{\gamma}_{\text{nonrad}}\tau - \tilde{\Phi}_1^{(2)}]\frac{t}{\tau}} e^{i\tilde{\Phi}_2^{(2)}\frac{t}{\tau}}. \end{aligned} \quad (57)$$

The oscillating part $e^{i\tilde{\Phi}_2^{(2)}\frac{t}{\tau}}$ is absorbed into the term oscillating at the atomic resonant frequency $e^{-i(\omega_0 - \tilde{\Delta})t}$ and provides correction to the polaron shift $\tilde{\Delta}$. The absorption spectrum is now easy to obtain as the imaginary part of the Fourier transform of the dipole autocorrelation function Eq. (57) and is a Lorentzian with width $\frac{(\tilde{\gamma}_{\text{nonrad}}\tau - \tilde{\Phi}_1^{(2)})}{\tau}$. Combining the short-time and long-time dynamics of the phonon correlation function, we conclude that the overall line shape exhibits Lorentzian behavior near the peak of the spectrum and decays more rapidly as a Gaussian in the wings.

We now consider population decay dynamics of the two-level atom coupled to the radiation reservoir and in the presence of direct nonradiative decay term H_{decay} . The nonequilibrium correlation function $\langle \hat{C}_+(t) \hat{\sigma}_{eg}(t) \hat{C}_-(t') \hat{\sigma}_{ge}(t') \rangle$ in Eq. (26), in the presence of nonradiative decay, can be expressed as

$$\begin{aligned} \langle \hat{C}_+(t) \hat{\sigma}_{eg}(t) \hat{C}_-(t') \hat{\sigma}_{ge}(t') \rangle \\ \simeq e^{-[\tilde{\Phi}(0) - \tilde{\Phi}(t-t')] - \tilde{\gamma}_{\text{nonrad}}(t-t')} \langle \hat{\sigma}_{eg}(t) \hat{\sigma}_{ge}(t') \rangle, \end{aligned} \quad (58)$$

where we have used $\langle \hat{C}_+(t) \hat{C}_-(t') \rangle = e^{-(\tilde{\Phi}(0) - \tilde{\Phi}(t-t')) - \tilde{\gamma}_{\text{nonrad}}(t-t')}$ [45]. Using the Born approximation described in

Eqs. (26)–(28) and replacing the atomic transition frequency $\omega'_0 \rightarrow \omega'_0 + i\gamma_{\text{nonrad}}$ [see discussion after Eq. (41)], we obtain

$$\langle \hat{\sigma}_{eg}(t) \hat{\sigma}_{ge}(t') \rangle \simeq e^{i\omega'_0(t-t')} e^{-\gamma_{\text{nonrad}}(t-t')} \langle \hat{\sigma}_{eg}(t') \rangle, \quad (59)$$

where $\omega'_0 = \omega_0 - \tilde{\Delta}$. Using Eqs. (59) and (58), Eq. (29) for $\ell(t)$ now has the form:

$$\begin{aligned} \frac{\partial \ell(t)}{\partial t} = -2\gamma_{\text{nonrad}} \ell(t) - \sum_k |\lambda_k|^2 \\ \times \int_0^t dt' e^{-(\gamma_{\text{nonrad}} + \tilde{\gamma}_{\text{nonrad}})(t-t') - (\tilde{\Phi}(0) - \tilde{\Phi}(t-t'))} \ell(t') \\ \times e^{i(\omega'_0 - \omega_k)(t-t')} + \text{c.c.} \end{aligned} \quad (60)$$

In the presence of nonradiative decay, Eq. (29) now has an additional contribution on the right-hand side given by $-\sum_p (1 + 2n_p) |\zeta_p|^2 \int_0^t dt' \ell(t') e^{i(\omega'_0 - \xi_p)(t-t')}$, where ξ_p is the dispersion of this additional decay channel [see Eq. (41)]. In the Markovian approximation, we write $\sum_p (1 + 2n_p) |\zeta_p|^2 \int_0^t dt' \ell(t') e^{i(\omega'_0 - \xi_p)(t-t')} \simeq 2\gamma_{\text{nonrad}} \ell(t)$ and obtain Eq. (60). Note that in the limit when $\lambda_k \rightarrow 0 \forall k$ (no radiative coupling), the population decays due to the first term on the right-hand side which arises due to the additional decay Hamiltonian Eq. (41).

Using a simple scaling analysis, it is easy to show that, for $t \ll \alpha^{-1}$, Eq. (60) simplifies to

$$\frac{\partial \ell(t)}{\partial t} = -2\gamma_{\text{nonrad}} \ell(t), \quad (61)$$

and the only decay mechanism for population is through the direct nonradiative decay term since the second term on the right-hand side does not contribute at these timescales. For $t \simeq \alpha^{-1}$, we now use the asymptotic expansion of $\tilde{\Phi}(t)$ (valid for $t \gg \tau$) outlined in Eqs. (55) and (56). Equation (60) can then be rewritten as

$$\begin{aligned} \frac{\partial \ell(t)}{\partial t} \simeq -2\gamma_{\text{nonrad}} \ell(t) - e^{-\tilde{\Phi}_1(0)} \sum_k |\lambda_k|^2 \int_0^t dt' \\ \times e^{-i\tilde{\Phi}_2(0)} e^{-\tilde{\gamma}_{\text{nonrad}}(t-t')} \ell(t') e^{i(\omega'_0 - \omega_k)(t-t')} + \text{c.c.}, \end{aligned} \quad (62)$$

where $\bar{\gamma}_{\text{nonrad}} = \gamma_{\text{nonrad}} + \tilde{\gamma}_{\text{nonrad}} - \frac{\tilde{\Phi}_1^{(2)}}{\tau}$, $\bar{\Phi}_1(0) = \tilde{\Phi}_1(0) - \tilde{\Phi}_1^{(1)}(0)$, and $\bar{\Phi}_2(0) = \tilde{\Phi}_2(0) - \tilde{\Phi}_2^{(1)}(0)$, and we have absorbed the term $e^{i\tilde{\Phi}_2^{(2)}\frac{t-t'}{\tau}}$ in $e^{i\omega'_0(t-t')}$. Note that the dot-photon coupling constant is now modified in the presence of direct nonradiative decay as $|\lambda_k|^2 \rightarrow e^{-\tilde{\Phi}_1(0)} |\lambda_k|^2$. Also $e^{-\tilde{\Phi}_1(0)} \sum_k |\lambda_k|^2 e^{i(\omega'_0 - \omega_k)(t-t')}$ is the phonon-renormalized radiative memory kernel where $e^{-\tilde{\Phi}_1(0)}$ is the effective Franck-Condon factor which renormalizes the dot-photon coupling. We note that the nonradiative decay channel leads to weakening of the photon memory because of the exponential damping term $e^{-\tilde{\gamma}_{\text{nonrad}}(t-t')}$. Using the isotropic dispersion relation Eq. (30) for the structured reservoir of a photonic crystal, Eq. (62) can be solved by Laplace transformation [38] to yield

$$\tilde{\ell}(s) = \frac{\ell(0)}{s + 2\gamma_{\text{nonrad}} + 2\text{Re}\tilde{Z}(s)}, \quad (63)$$

where $\tilde{Z}(s) = e^{-\tilde{\Phi}_1(0)} \frac{\alpha^{\frac{3}{2}} e^{\frac{i\pi}{4}} e^{-i\tilde{\Phi}_2(0)}}{\sqrt{s + i\delta + \tilde{\gamma}_{\text{nonrad}}}}$. The photonic memory of the structured reservoir is now damped, and the two-level

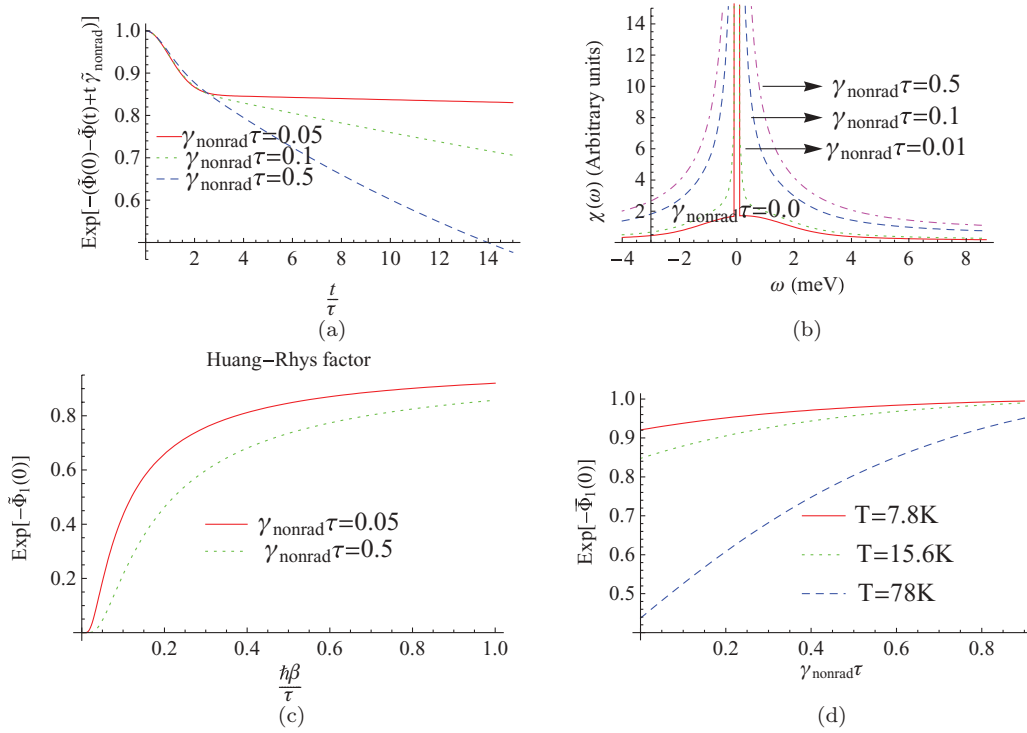


FIG. 2. (Color online) Salient features of the modified undamped acoustic phonon correlation function in the presence of direct nonradiative decay $e^{-(\tilde{\Phi}(0)-\tilde{\Phi}(t)+t\tilde{\gamma}_{\text{nonrad}})}$, where $\tilde{\Phi}(t)$ and $\tilde{\gamma}_{\text{nonrad}}$ are defined in Eqs. (49) and (51), respectively. In (a), we plot the modified phonon correlation as a function of $\frac{t}{\tau}$, which now decays at long times due to direct nonradiative decay. In (b), we plot the spectral profile corresponding to (a). The δ -function peak in the middle acquires a width for finite nonradiative decay rate. The zero-phonon line resembles a Lorentzian for large γ_{nonrad} . The width of the Lorentzian also increases with γ_{nonrad} . The large ω (small t) Gaussian spectrum persists in the presence of direct nonradiative decay. In (c), we plot the spectral weight of the zero-phonon line given by $e^{-\tilde{\Phi}(0)}$ as a function of inverse-temperature. The spectral weight decreases with increasing temperature due to excitation of the sidebands. Finally in (d), we study the Franck-Condon shift $e^{-\tilde{\Phi}(0)}$ (see discussion following Eq. (62)) of the excited state as a function of direct nonradiative decay. Increasing $\gamma_{\text{nonrad}}\tau$ reduces the Franck-Condon shift. The artificial subnatural linewidth of the radiative transition is thereby removed.

system does not support a steady-state population. The atom decays nonradiatively at a rate determined by $\tilde{\gamma}_{\text{nonrad}}$ and γ_{nonrad} in spite of the presence of a photonic band gap.

The polarization dynamics of a quantum dot in a PBG material and coupled to an acoustic phonon reservoir with nonradiative decay is easy to obtain by using the modified phonon correlation function:

$$P_{MF}(t) \simeq -i\Theta(t)e^{-i\omega_e t - \gamma_{\text{nonrad}} t - \tilde{\gamma}_{\text{nonrad}} t} e^{-(\tilde{\Phi}(0)-\tilde{\Phi}(t))} \times \left[2a_1 x_1 e^{\alpha x_1^2 t} + a_2 x_2 e^{\alpha x_2^2 t} + a_2 y_2 e^{\alpha x_2^2 t} - \sum_{j=1}^3 a_j y_j \text{Erfc}(\sqrt{\alpha x_j^2 t}) e^{\alpha x_j^2 t} \right]. \quad (64)$$

The definition of constants a_i 's and x_i 's can be found in [8]. The radiative timescale is now determined by $\alpha^{\frac{3}{2}} = \frac{e^{-\tilde{\Phi}(0)} \omega_0^{\frac{3}{2}} |D_{ge}|^2}{6\pi\epsilon_0 \hbar c^3}$. The detuning of the quantum dot transition frequency is given by $\delta = \omega_0 - \tilde{\Delta} - \omega_e$. There is no long-term coherence trapped in the photon-atom bound state which, at $t \gg \tau$, decays at a rate $\gamma_{\text{nonrad}} + \tilde{\gamma}_{\text{nonrad}} - \frac{\tilde{\Phi}(0)}{\tau}$.

In Fig. 2, we plot important features of the modified phonon correlation function $e^{-(\tilde{\Phi}(0)-\tilde{\Phi}(t)+t\tilde{\gamma}_{\text{nonrad}})}$ in the presence of

direct nonradiative decay, where $\tilde{\Phi}(t)$ and $\tilde{\gamma}_{\text{nonrad}}$ are defined in Eqs. (49) and (51), respectively. In Fig. 2(a), we plot the modified phonon correlation as a function of $\frac{t}{\tau}$. Note that the correlation function now decays at long times. In Fig. 2(b), we plot the absorption spectrum which is the Fourier transform of the modified phonon correlation function $e^{-(\tilde{\Phi}(0)-\tilde{\Phi}(t)+t\tilde{\gamma}_{\text{nonrad}})}$. The zero-phonon line is now broadened due to nonradiative decay and the spectrum acquires a finite linewidth. For large γ_{nonrad} , the spectrum is almost Lorentzian for ω (or large t) in the vicinity of the resonant frequency. We also plot the spectral weight of the zero-phonon line given by $e^{-\tilde{\Phi}(0)}$ as a function of inverse-temperature $\frac{\hbar\beta}{\tau}$. The zero-phonon line intensity decreases with increasing temperature due to transfer of spectral weight to the sidebands and the decay of the phonon correlation function. The Franck-Condon displacement of the excited state wave function, $e^{-\tilde{\Phi}(0)}$ [see discussion following Eq. (62)], is also studied as a function of direct nonradiative decay. Increasing $\gamma_{\text{nonrad}}\tau$ reduces the Franck-Condon shift and the artificial subnatural linewidth of the radiative transition approaches the natural width.

In Fig. 3, we study the influence of nonradiative decay on quantum dot polarization $|P_{MF}(t)|$ [Eq. (64)] and on the excited-state population $l(t)$ described by Eq. (63) in the structured reservoir of a photonic crystal for various

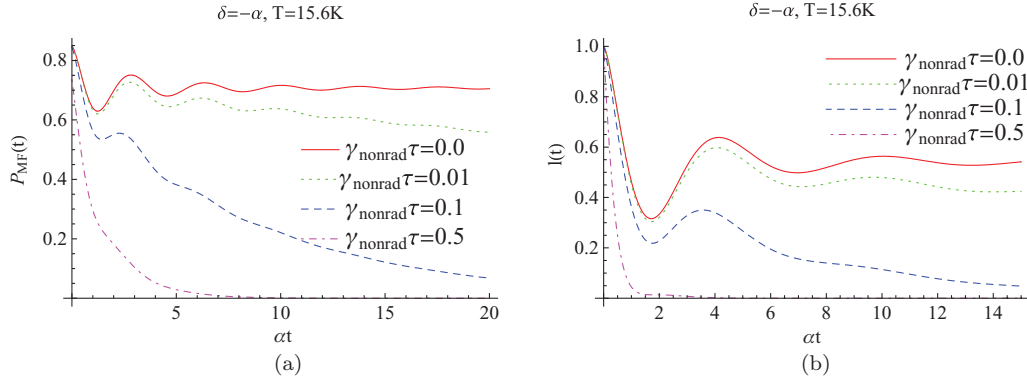


FIG. 3. (Color online) Study of the influence of nonradiative decay on quantum dot dipole autocorrelation function (polarization) $|P_{MF}(t)|$ [Eq. (64)] and the excited-state population $I(t)$ [Eq. (63)] in a photonic crystal for detuning $\delta/\alpha = -1$ from the photonic band edge. The timescale is measured in units of α^{-1} , where $\alpha = 10^{10}\text{s}^{-1}$ for $\omega_0 \simeq 10^{15}\text{s}^{-1}$. In (a), we depict the polarization dynamics. In (b), we plot the excited-state population dynamics. The rapid loss of coherence at picosecond timescales in (a) appears as a nearly discontinuous drop near $t = 0$ on the timescale depicted. There is no long-time coherence trapped in the photon-atom bound state and no fractionalized steady-state population in the presence of direct nonradiative decay even though the quantum dot transition is inside the photonic band gap.

detunings of the atomic transition frequency from the photonic band edge. There is no long-time coherence trapped in the photon-atom bound state and no fractionalized steady-state population in the presence of direct nonradiative decay for all values of detuning δ .

C. Line shape and population decay for damped acoustic phonons

The model Hamiltonian Eq. (1) describes purely radiative decay from each of the dressed states (phonon sidebands). In an ordinary vacuum, this radiative decay is possible from all the dressed states. The linewidth of any given sideband is artificially found to be subnatural. The Franck-Condon displacement of the excited-state wave function (with a phonon cloud surrounding the excited-state quantum dot) diminishes the transition rate from each dressed state. For a quantum dot in ordinary vacuum, coupled to a continuum of undamped acoustic phonons, the subnatural linewidth of individual sidebands leads to a reduced decay rate. In a PBG material, where radiative decay can be completely suppressed over certain spectral ranges, the model Hamiltonian Eq. (1) leads to the untenable result that the lifetime of the photon-atom bound state is increased by phonon interactions. In Sec. VI B, we introduced an independent nonradiative decay mechanism to correct this picture. In this subsection, we demonstrate how the inclusion of a finite phonon lifetime leads to a more realistic picture of the phonon sideband linewidth and decay of the photon-atom bound state. Our phenomenological phonon damping parameter captures processes like inelastic scattering of phonons and other anharmonic processes that allow the phonons in the polaronic cloud to decay into lower energy phonons and for energy to be dissipated within the vibrational degrees of freedom into a thermal heat bath.

We introduce a phenomenological phonon decay rate γ_q into the phonon propagator as follows [35]:

$$iD(t) = \sum_q \eta_q^2 [N_q e^{(i\Omega_q - \gamma_q)|t|} + (N_q + 1)e^{(-i\Omega_q - \gamma_q)|t|}]. \quad (65)$$

The self-energy contribution can again be evaluated using the linked cluster theorem, and we find a modified $\tilde{\Phi}(t)$ now given by

$$\tilde{\Phi}(t) = \sum_q \eta_q^2 \left[\frac{N_q}{(\Omega_q + i\gamma_q)^2} e^{(i\Omega_q - \gamma_q)t} + \frac{N_q + 1}{(\Omega_q - i\gamma_q)^2} e^{(-i\Omega_q - \gamma_q)t} \right]. \quad (66)$$

This is identical to Eq. (46b) except with the single nonradiative decay rate γ_{nonrad} replaced with a set of phonon damping coefficients $\{\gamma_q\}$. As before we write $\tilde{\Phi}(t) = \tilde{\Phi}_1(t) + i\tilde{\Phi}_2(t)$. Also $\tilde{\Phi}(0)$ can be decomposed as $\tilde{\Phi}(0) = \tilde{\Phi}_1(0) + i\tilde{\Phi}_2(0)$, where $e^{-\tilde{\Phi}_1(0)}$ is the intensity of the zero-phonon line (Huang-Rhys factor) and $\tilde{\Phi}_2(0)$ is an additional phase:

$$\tilde{\Phi}_1(0) = \sum_q \eta_q^2 \frac{\Omega_q^2 - \gamma_q^2}{(\Omega_q^2 + \gamma_q^2)^2} (1 + 2N_q), \quad (67a)$$

$$\tilde{\Phi}_2(0) = \sum_q \eta_q^2 \frac{2\Omega_q \gamma_q}{(\Omega_q^2 + \gamma_q^2)^2}. \quad (67b)$$

Also $\tilde{\Phi}'(0) = \Gamma_{\text{damp}} - i\tilde{\Delta}$, where Γ_{damp} is an additional decay term contributing to the polarization decay due to phonon damping and $\tilde{\Delta}$ is the modified polaron shift. They are given by

$$\Gamma_{\text{damp}} = \sum_q \frac{\eta_q^2 \gamma_q}{\Omega_q^2 + \gamma_q^2} (1 + 2N_q), \quad (68)$$

$$\tilde{\Delta} = \sum_q \eta_q^2 \frac{\Omega_q}{\Omega_q^2 + \gamma_q^2}.$$

For analytical simplicity, we consider a solvable model and assume that the phonon damping is wave-vector dependent and has the form $\gamma_q = \gamma\Omega_q$, where γ is a real number between zero and one. The most efficient of anharmonic three-phonon processes, the Landau-Rumer process of relaxation of a transverse acoustic mode into thermal longitudinal modes, has

a dependence of this form [54,55]:

$$\gamma_q = \frac{6G^2(k_B T)^4 \left(1 + \frac{2c_l}{3c_t}\right)}{\pi \rho c_T c_l^4 \hbar^3} \Omega_q, \quad (69)$$

where c_t (c_l) is the transverse (longitudinal) sound velocity and G is the Gruneissen constant (taken to be 2).

The modified phonon correlation function due to phonon damping can be easily evaluated using Eqs. (65) and (43) for $W(t)$ and is given by [in the approximation $\coth\left(\frac{\hbar\beta x}{2\tau}\right) \simeq \frac{2\tau}{\hbar\beta x}$]:

$$W(t) = \alpha_p \int_0^t dt_1 \int_0^{t_1} dt_2 \int_0^\infty dx x^3 \exp\left(-\frac{x^2}{2}\right) \left[i \sin(x\bar{t}_{12}) - \frac{2\tau}{\hbar\beta x} \cos(x\bar{t}_{12}) \right] e^{-\gamma x \bar{t}_{12}}, \quad (70)$$

where $\bar{t}_{12} = \frac{t_1 - t_2}{\tau}$. This differs from the case of direct nonradiative decay Eq. (48) through the appearance of the dimensionless wave vector of the damped acoustic phonons in the final temporal exponential. The function $W(t)$ is easily evaluated and is given by

$$W(t) = -\alpha_p^{(1)} \times \frac{(1 - \gamma^2) + \sqrt{\frac{2}{\pi}} \bar{t} \gamma (1 + \gamma^2) + (1 + \gamma^2)^2 \text{Re} \left[\frac{e^{z^2} \text{Erfc}[z]}{(-i + \gamma)^2} \right]}{(1 + \gamma^2)^2} + i \alpha_p^{(2)} \bar{t} \frac{-1 + (1 + \gamma^2) \text{Im} \left[\frac{e^{z^2} \text{Erfc}[z]}{-i + \gamma} \right]}{(1 + \gamma^2)}, \quad (71)$$

where $z = \frac{(-i + \gamma)\bar{t}}{\sqrt{2}}$, $\alpha_p^{(1)} = \frac{\sqrt{2\pi} \alpha_p \tau}{\hbar\beta}$, and $\alpha_p^{(2)} = \sqrt{\frac{\pi}{2}} \alpha_p$. The modified phonon correlation function from Eq. (71) is straightforward to obtain:

$$\tilde{\Phi}_1(t) = -\alpha_p^{(1)} \text{Re} \left[\frac{e^{z^2} \text{Erfc}[z]}{(-i + \gamma)^2} \right], \quad (72a)$$

$$\tilde{\Phi}_2(t) = \alpha_p^{(2)} \bar{t} \text{Im} \left[\frac{e^{z^2} \text{Erfc}[z]}{(-i + \gamma)} \right]. \quad (72b)$$

The zero-phonon line spectral weight $e^{-\tilde{\Phi}_1(0)}$ which is determined by $\tilde{\Phi}_1(0) = \alpha_p^{(1)} \frac{(1 - \gamma^2)}{(1 + \gamma^2)^2}$ and the phase $\tilde{\Phi}_2(0) = 0$. The linear decay contribution Γ_{damp} and the modified polaron shift $\tilde{\Delta}$ are now given by

$$\Gamma_{\text{damp}} \tau = \alpha_p^{(1)} \sqrt{\frac{2}{\pi}} \frac{\gamma}{1 + \gamma^2}, \quad (73a)$$

$$\tilde{\Delta} \tau = \alpha_p^{(2)} \frac{1}{1 + \gamma^2}. \quad (73b)$$

The short-time $t \ll \tau$ phonon dynamics contained in $e^{-[\tilde{\Phi}(0) - \tilde{\Phi}(t) + t\tilde{\Phi}'(0)]}$ is identical to the case of direct nonradiative decay obtained previously in Eq. (53). The wings of the spectrum are Gaussian with width $D^2 = \frac{\alpha_p^{(1)}}{\tau^2}$. It is instructive to note that the short-time phonon dynamics is independent of the nature of phonon damping or direct nonradiative decay. In fact it is identical to the case of undamped phonons. To see this, we observe that $e^{-[\tilde{\Phi}(0) - \tilde{\Phi}(t) + t\tilde{\Phi}'(0)]} \simeq e^{\frac{t^2}{2} \tilde{\Phi}''(0)}$. Using the general expressions for $\tilde{\Phi}(t)$ obtained in Eq. (37) for undamped phonons, Eq. (46b) for direct nonradiative decay, and Eq. (66)

for damped phonons, we find

$$\begin{aligned} \tilde{\Phi}''(0) &= - \sum_q \eta_q^2 (1 + 2N_q) \\ &= - \frac{2\alpha_p}{\hbar\beta\tau} \int_0^\infty dx x^2 e^{-\frac{x^2}{2}} \\ &= - \frac{\alpha_p^{(1)}}{\tau^2}. \end{aligned} \quad (74)$$

This can also be verified using explicit expressions for $\tilde{\Phi}(t)$ obtained in Eq. (49) for direct nonradiative decay and Eq. (72) for damped phonons.

In the long-time $t \gg \tau$ regime, the error functions in Eq. (72) for $\tilde{\Phi}_1(t)$ and $\tilde{\Phi}_2(t)$ can be replaced, to a very good approximation, by

$$\text{Erfc}[z] \simeq \frac{e^{-z^2}}{\sqrt{\pi}z} \quad (|z| \gg 1). \quad (75)$$

Equation (72) for $\tilde{\Phi}_1(t)$ and $\tilde{\Phi}_2(t)$ then has a simple form:

$$\tilde{\Phi}_1(t) \simeq \alpha_p^{(1)} \frac{\sqrt{\frac{2}{\pi}} \gamma (3 - \gamma^2)}{\bar{t} (1 + \gamma^2)^3} \quad (\bar{t} \gg 1), \quad (76a)$$

$$\tilde{\Phi}_2(t) = -\alpha_p^{(2)} \frac{2\sqrt{\frac{2}{\pi}} \gamma}{(1 + \gamma^2)^2} \quad (\bar{t} \gg 1). \quad (76b)$$

Using the fact that $\tilde{\Phi}_1(t) \rightarrow 0$ for $\bar{t} \gg 1$ and neglecting the time-independent factor $\tilde{\Phi}_2(t)$, we approximate $e^{-[\tilde{\Phi}(0) - \tilde{\Phi}(t) + t\tilde{\Phi}'(0)]}$ [using $\tilde{\Phi}_2(0) = 0$; see Eq. (72)] by $e^{-\tilde{\Phi}_1(0) - t\tilde{\Phi}'(0)}$. It follows that for $\bar{t} \gg 1$ [using $\tilde{\Phi}'(0) = \Gamma_{\text{damp}} - i\tilde{\Delta}$ and Eq. (73) for Γ_{damp}]:

$$e^{-[\tilde{\Phi}(0) - \tilde{\Phi}(t) + t\tilde{\Phi}'(0)]} \simeq e^{-\tilde{\Phi}_1(0) + i\tilde{\Delta}t} e^{-\frac{2\alpha_p\gamma}{\hbar\beta(1+\gamma^2)} \bar{t}}. \quad (77)$$

The spectrum (Fourier transform of the dipole autocorrelation function) clearly exhibits a Lorentzian peak with linewidth $\frac{2\alpha_p\gamma}{(1+\gamma^2)} \frac{K_B T}{(\hbar/\tau)}$. As $\gamma \rightarrow 0$, the Lorentzian peak transforms to a delta-function centered at the atomic transition frequency with a broad Gaussian background as in the case of undamped acoustic phonons (see Sec. V A). The zero-phonon line is unbroadened in the absence of phonon damping, which is characteristic of pure dephasing.

The atomic dipole autocorrelation function in the structured reservoir of a photonic crystal is now given by

$$\begin{aligned} P_{MF}(t) &\simeq -i\Theta(t) e^{-i\omega_e t - \Gamma_{\text{damp}} t} e^{-[\tilde{\Phi}(0) - \tilde{\Phi}(t)]} \\ &\times \left[2a_1 x_1 e^{\alpha x_1^2 t} + a_2 (x_2 + y_2) e^{\alpha x_2^2 t} \right. \\ &\left. - \sum_{j=1}^3 a_j y_j \text{Erfc}(\sqrt{\alpha x_j^2 t}) e^{\alpha x_j^2 t} \right]. \end{aligned} \quad (78)$$

The definition of constants a_i 's and x_i 's can be found in [8]. Γ_{damp} and $\tilde{\Delta}$ are defined in Eq. (43) and $\tilde{\Phi}(t)$ is defined in Eq. (72). Note that the photon-atom bound state loses all polarization on the timescale $\Gamma_{\text{damp}}^{-1}$.

We now consider the population decay dynamics of the excited state in the presence of acoustic phonon damping. The nonequilibrium correlation function

$\langle \hat{C}_+(t) \hat{\sigma}_{eg}(t) \hat{C}_-(t') \hat{\sigma}_{ge}(t') \rangle$ in Eq. (26), in the presence of phonon damping, can be expressed as

$$\begin{aligned} & \langle \hat{C}_+(t) \hat{\sigma}_{eg}(t) \hat{C}_-(t') \hat{\sigma}_{ge}(t') \rangle \\ & \simeq e^{-[\tilde{\Phi}(0) - \tilde{\Phi}(t-t')] e^{-\Gamma_{\text{damp}}(t-t')}} \langle \hat{\sigma}_{eg}(t) \hat{\sigma}_{ge}(t') \rangle, \end{aligned} \quad (79)$$

where we have used $\langle \hat{C}_+(t) \hat{C}_-(t') \rangle = e^{-[\tilde{\Phi}(0) - \tilde{\Phi}(t-t')] e^{-\Gamma_{\text{damp}}(t-t')}} [45]$. In the Born approximation as in Eq. (28), Eq. (79) can be simplified as

$$\begin{aligned} & \langle \hat{C}_+(t) \hat{\sigma}_{eg}(t) \hat{C}_-(t') \hat{\sigma}_{ge}(t') \rangle \\ & \simeq e^{-[\tilde{\Phi}(0) - \tilde{\Phi}(t-t')] e^{i\omega'_0(t-t') - \Gamma_{\text{damp}}(t-t')}} \langle \hat{\sigma}_{ee}(t') \rangle. \end{aligned} \quad (80)$$

Using Eq. (76) in Eq. (80) and noting that $\tilde{\Phi}_2(0) = 0$, $\tilde{\Phi}_1(t) \rightarrow 0$ for $t \gg \tau$, and $e^{-i\tilde{\Phi}_2(t)} \simeq 1$, Eq. (29) for $\ell(t)$ for long timescales is governed by the integro-differential equation:

$$\begin{aligned} \frac{\partial \ell(t)}{\partial t} & \simeq -e^{-\tilde{\Phi}_1(0)} \sum_k |\lambda_k|^2 \\ & \times \int_0^t dt' e^{-\Gamma_{\text{damp}}(t-t')} \ell(t') e^{i(\omega'_0 - \omega_k)(t-t')} + \text{c.c.} \end{aligned} \quad (81)$$

Solving Eq. (81) for the structured reservoir of a photonic crystal using the isotropic dispersion model of Eq. (30), we find $\tilde{l}(s) = \frac{l(0)}{s + 2\text{Re}\tilde{Z}(s)}$, where

$$\tilde{Z}(s) = \frac{\alpha^{\frac{3}{2}} e^{\frac{i\pi}{4}} e^{-\tilde{\Phi}_1(0)}}{\sqrt{s + i\delta + \Gamma_{\text{damp}}}}. \quad (82)$$

We note that in spite of the absence of any direct nonradiative decay channel, the atom does not have a steady-state population even if the atomic transition frequency is inside the photonic band gap and decays at long times at a rate determined by Γ_{damp} . For example, if we consider the regime $\Gamma_{\text{damp}} \gg \delta$, then $\tilde{l}(s) \simeq \ell(0)/(s + \gamma_{ph})$, where $\gamma_{ph} \simeq e^{-\tilde{\Phi}_1(0)} \sqrt{\frac{2\alpha^3}{\Gamma_{\text{damp}}}}$. It follows that $\ell(t) \simeq \ell(0)e^{-\gamma_{ph}t}$ for long timescales. Hence, there is no fractionalized steady state irrespective of the sign of δ . Unlike the case of purely nonradiative decay (where decay occurs independently of radiative coupling), our phonon damping scales with the strength of the radiative coupling constant. Phonon damping may be regarded as a vital correction to our mean-field description Eq. (8) of the quantum dot dressed by phonons. In this mean-field theory, we neglected decay of the atomic polarization by the simultaneous emission of photons and phonons. The various phonon sidebands were only allowed to decay by purely radiative emission (with a Franck-Condon displaced radiative coupling coefficient). Our phenomenological phonon damping process now describes the phonon-assisted decay of the atomic polarization. Phonon damping also provides a cutoff to the extent of Franck-Condon displacement of the excited state (atom plus acoustic phonons) wave function.

In Fig. 4, we study characteristic features of the modified phonon correlation function $e^{-[\tilde{\Phi}(0) - \tilde{\Phi}(t) + \Gamma_{\text{damp}}t]}$ in the presence of phonon damping, where $\tilde{\Phi}(t)$ and Γ_{damp} are defined in Eqs. (72) and (73), respectively. The modified phonon correlation function decays at long times due to the finite lifetime of phonons. The zero-phonon line now acquires a finite width $\frac{2\alpha_p\gamma}{(1+\gamma^2)} \frac{K_B T}{(\hbar/\tau)}$ due to phonon damping. We also study

the influence of finite phonon lifetimes on quantum dot polarization $|P_{MF}(t)|$ [Eq. (78)] and the excited-state population $l(t)$ [Eq. (82)] in the structured reservoir of a photonic crystal for detuning $\delta/\alpha = -1$ of the atomic transition frequency from the photonic band edge. No long-time coherence is trapped in the photon-atom bound state, and the population decays to zero at a rate determined by the lifetime of the phonons surrounding the quantum dot.

VI. DISCUSSION

In this article, we have presented a mean-field theory for the role of phonons in modifying the optical properties of two-level systems. Using a thermodynamic Green's function formalism, the combined effect of photon and phonon reservoirs was shown to provide dressing of the atomic states with various numbers of phonons and the optical absorption spectrum was shown to consist of transitions between the atomic ground state and various dressed excited states (phonon sidebands). In our mean-field theory, the lattice displacement operator was replaced by an equilibrium thermal average over the phonon reservoir. This led to an effective temperature-dependent radiative coupling constant describing the (Franck-Condon) overlap between the displaced excited state and the ground state. In this mean-field theory, phonon-assisted decay of the atomic polarization was removed from the Hamiltonian. The linewidth of each dressed state was determined entirely by the Franck-Condon displaced optical transition dipole matrix element and the electromagnetic density of states at the dressed state frequency. Phonon-assisted decay processes were then introduced through a phenomenological phonon damping parameter, providing a more realistic linewidth to the phonon sidebands and regulating the extent of Franck-Condon displacement. In the case of undamped optical phonons, the line shape comprises distinct peaks separated by an optical phonon frequency with the linewidth of a sideband determined solely by the reduced transition matrix element and the electromagnetic density of states at the corresponding sideband frequency. When phonon damping is introduced, the sidebands are broadened and a realistic picture is obtained. This additional broadening is governed by the lifetime of optical phonons. Undamped acoustic phonons produce a Gaussian spectral function with a sharp peak for the zero-phonon line. For a thermal reservoir of damped acoustic phonons, the zero-phonon line is broadened, resulting in a Lorentzian structure in the vicinity of the atomic transition frequency and Gaussian wings away from the transition.

The polarization dynamics of the quantum dot was studied using the temporal dipolar autocorrelation function. The autocorrelation function was evaluated using the mean-field factorization described earlier. For a phonon reservoir consisting of undamped acoustic phonons coupled linearly to the quantum dot population operator (Independent-Boson model), the role of phonons was limited to pure dephasing. In an unstructured electromagnetic reservoir, the phonons cause a rapid initial partial dephasing on picosecond timescales as the polaronic cloud forms. On longer timescales, the polarization decays exponentially to zero through electromagnetic dephasing. We then generalized the system to include nonradiative decay processes and damped phonons. Direct nonradiative decay

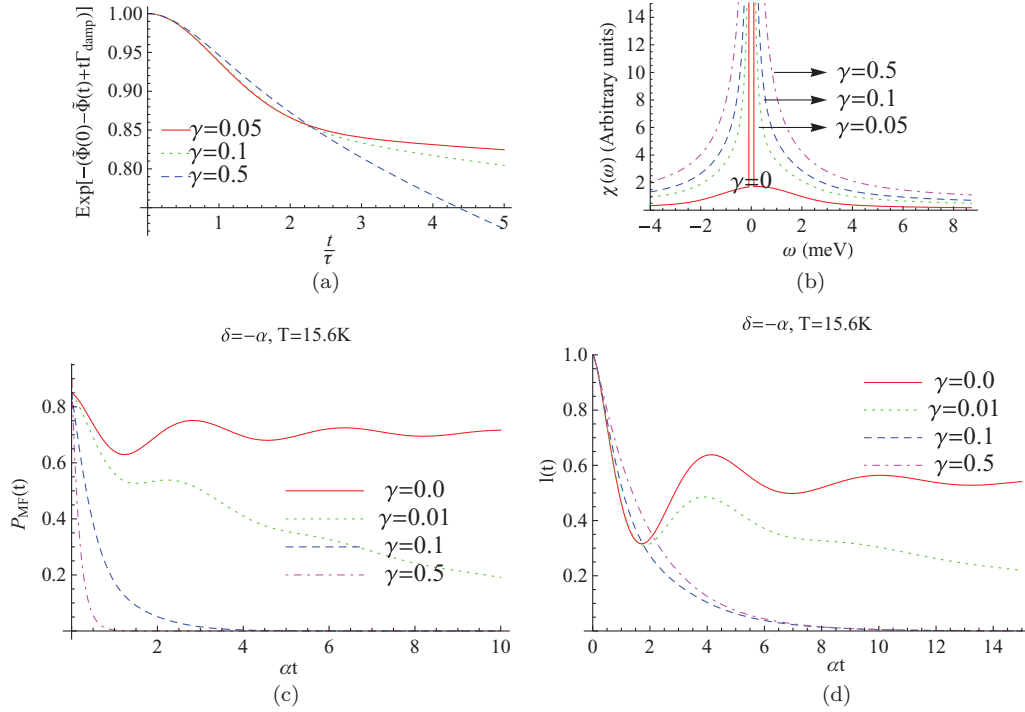


FIG. 4. (Color online) Salient features of the modified acoustic phonon correlation function in the presence of phonon damping $e^{-(\tilde{\Phi}(0)-\tilde{\Phi}(t)+t\Gamma_{\text{damp}})}$, where $\tilde{\Phi}(t)$ and Γ_{damp} are defined in Eqs. (72) and (73), respectively. In (a), we plot the modified phonon correlation as a function of $\frac{t}{\tau}$. The correlation function decays at long times due to the finite lifetime of phonons. In (b), we plot the spectral profile corresponding to (a). The δ -function peak in the middle acquires a width for finite phonon damping. The zero-phonon line resembles a Lorentzian for large phonon damping γ , and its width increases with increasing γ . The large ω (small t) Gaussian spectrum remains as in the case of undamped acoustic phonons. In (c) and (d), we study the influence of finite acoustic phonon lifetimes on the quantum dot dipole autocorrelation function (polarization) $|P_{MF}(t)|$ [Eq. (78)] and the excited state population $l(t)$ [Eq. (82)] in a photonic crystal for detuning $\delta/\alpha = -1$ of the quantum dot transition frequency from the photonic band edge. The timescale is measured in units of α^{-1} , where $\alpha = 10^{10} \text{ s}^{-1}$ for $\omega_0 \simeq 10^{15} \text{ s}^{-1}$. No long-time coherence is trapped in the photon-atom bound state, and no fractionalized steady-state population is found with finite phonon lifetimes even though the quantum dot transition is inside the photonic band gap.

is beyond the framework of our starting Hamiltonian and corresponds to the direct coupling of phonon operators to the quantum dot dipole. Polarization decay beyond pure dephasing was obtained using a semi-phenomenological model for non-radiative relaxation. Atomic polarization decays exponentially to zero at a faster rate involving the sum of nonradiative decay rate, the phonon damping rate, and the electromagnetic dephasing rate. The overall rate of decay increases with temperature and the nonradiative coupling strength.

For a quantum dot placed inside a photonic crystal and coupled to a bath of undamped acoustic phonons, the long-time polarization may be nonzero because of the formation of a photon-atom bound state. A rapid decay of polarization at very small timescales occurs as the polaronic cloud forms. This nonzero residual coherence may be of importance for quantum information-processing applications. However, when nonradiative decay and damped phonons are included, there is no long-time residual coherence. The coherence trapped in the photon-atom bound state, in the case of pure dephasing, was shown to be controlled by the application of a coherent external laser field [13]. It is of considerable interest to determine whether suitable forms of external control can be adapted to maintain coherence in the photon-atom bound state when phonon damping and direct nonradiative decay are present.

In order to describe population dynamics of an excited quantum dot, we considered Heisenberg equations of motion for the relevant atomic operators. The hierarchy of equations of motion was closed using a mean-field factorization of the atomic and lattice operators and a Born approximation that collapses the resulting two-time nonequilibrium atomic dipole correlation function to the atomic population at single time. In the absence of nonradiative decay and phonon damping, the long-time excited-state population in a photonic crystal may be nonzero for negative detunings from the photonic band edge leading to the “fractionalized” steady state. In the case of undamped optical and acoustic phonons, the fractionalized steady-state population is artificially increased with increasing dot-phonon coupling strength and increasing temperature because of the polaron shift between the excited and ground states of the quantum dot. For acoustic phonons, there was substantial dephasing of the atomic transition dipole moment with increasing temperatures, contributing to residual population in the excited state. However, in the presence of nonradiative decay and phonon damping, there is no fractionalized steady state and the population decays to zero.

Our formalism can be generalized to multilevel atoms interacting simultaneously with electromagnetic and vibrational degrees of freedom. Coherent control of the polarization of a

three-level atom using an external laser field in the presence of pure dephasing can be described in this framework. Our formalism enables a more microscopic description than presented earlier [13] of the interplay between externally imposed coherence and various dephasing effects. Our formalism can also treat interactions between multiple quantum dots. Interacting quantum dots that are coupled to a common electromagnetic reservoir and correlated or uncorrelated phonon reservoirs are experimental systems of interest for quantum information processing. Decoherence of two entangled quantum dots placed in close proximity inside a PBG material can likewise be analyzed at a microscopic level using our method.

ACKNOWLEDGMENTS

This work was supported in part by the Natural Sciences and Engineering Research Council of Canada.

APPENDIX: PHONON SIDEBAND CONTRIBUTION TO MEAN-FIELD THERMODYNAMIC GREEN'S FUNCTION

Evaluating the commutator $[\hat{\sigma}_{ge}, H_{MF}]$ in Eq. (21) using the mean-field Hamiltonian Eq. (8), we find

$$[\hat{\sigma}_{ge}, H_{MF}] = (\omega_0 - \Delta)\hat{\sigma}_{ge} + \sum_k \tilde{\lambda}_k (\hat{\sigma}_{gg} - \hat{\sigma}_{ee})\hat{a}_k. \quad (\text{A1})$$

Using Eq. (A1), we find

$$\begin{aligned} (\omega - n\Omega_0)G_{\omega,n}^{MF}([\hat{\sigma}_{ge}, H_{MF}], \hat{\sigma}_{eg}) \\ = 1 + (\omega_0 - \Delta)G_{\omega,n}^{MF}(\hat{\sigma}_{ge}, \hat{\sigma}_{eg}) \\ + \sum_k \tilde{\lambda}_k G_{\omega,n}^{MF}[(\hat{\sigma}_{gg} - \hat{\sigma}_{ee})\hat{a}_k, \hat{\sigma}_{eg}]. \end{aligned} \quad (\text{A2})$$

In order to close the system of equations, we need to express $G_{\omega,n}^{MF}(\hat{\sigma}_{gg}\hat{a}_k, \hat{\sigma}_{eg})$ and $G_{\omega,n}^{MF}(\hat{\sigma}_{ee}\hat{a}_k, \hat{\sigma}_{eg})$ in terms of $G_{\omega,n}^{MF}(\hat{\sigma}_{ge}, \hat{\sigma}_{eg})$. The equation of motion for $G_{\omega,n}^{MF}(\hat{\sigma}_{ee}\hat{a}_k, \hat{\sigma}_{eg})$ is

$$\begin{aligned} (\omega - n\Omega_0)G_{\omega,n}^{MF}(\hat{\sigma}_{ee}\hat{a}_k, \hat{\sigma}_{eg}) \\ = \langle [\hat{\sigma}_{ee}\hat{a}_k(0), \hat{\sigma}_{eg}(0)] \rangle_{H_{MF}} + G_{\omega,n}^{MF}([\hat{\sigma}_{ee}\hat{a}_k, H_{MF}], \hat{\sigma}_{eg}). \end{aligned} \quad (\text{A3})$$

The first term on the right-hand side is identically zero. The commutator $[\hat{\sigma}_{ee}\hat{a}_k, H_{MF}]$ is

$$[\hat{\sigma}_{ee}\hat{a}_k, H_{MF}] = \omega_k \hat{\sigma}_{ee}\hat{a}_k + \sum_q \tilde{\lambda}_q \hat{\sigma}_{eg}\hat{a}_k\hat{a}_q - \sum_q \tilde{\lambda}_q^* \hat{\sigma}_{ge}\hat{a}_q^\dagger\hat{a}_k. \quad (\text{A4})$$

Using Eq. (A4) in Eq. (A3), we obtain an equation of motion for $G_{\omega,n}^{MF}(\hat{\sigma}_{ee}\hat{a}_k, \hat{\sigma}_{eg})$:

$$\begin{aligned} (\omega - n\Omega_0)G_{\omega,n}^{MF}(\hat{\sigma}_{ee}\hat{a}_k, \hat{\sigma}_{eg}) \\ = \omega_k G_{\omega,n}^{MF}(\hat{\sigma}_{ee}\hat{a}_k, \hat{\sigma}_{eg}) + \sum_q \tilde{\lambda}_q G_{\omega,n}^{MF}(\hat{\sigma}_{eg}\hat{a}_k\hat{a}_q, \hat{\sigma}_{eg}) \\ - \sum_q \tilde{\lambda}_q^* G_{\omega,n}^{MF}(\hat{\sigma}_{ge}\hat{a}_q^\dagger\hat{a}_k, \hat{\sigma}_{eg}). \end{aligned} \quad (\text{A5})$$

It is easy to see that the Green's functions $G_{\omega,n}^{MF}(\hat{\sigma}_{eg}\hat{a}_k\hat{a}_q, \hat{\sigma}_{eg})$ and $G_{\omega,n}^{MF}(\hat{\sigma}_{ge}\hat{a}_q^\dagger\hat{a}_k, \hat{\sigma}_{eg})$ generate equations of motion

involving higher powers of photon operators. In order to close this hierarchy of equations, we decouple the two-level system and photon operators in the Green's function by replacing the photon operators with their thermal expectation values evaluated in the absence of dot-photon interaction:

$$\begin{aligned} G_{\omega,n}^{MF}(\hat{\sigma}_{eg}\hat{a}_k\hat{a}_q, \hat{\sigma}_{eg}) &\simeq \delta_{kq} \langle \hat{a}_k\hat{a}_k \rangle G_{\omega,n}^{MF}(\hat{\sigma}_{eg}, \hat{\sigma}_{eg}), \\ G_{\omega,n}^{MF}(\hat{\sigma}_{ge}\hat{a}_q^\dagger\hat{a}_k, \hat{\sigma}_{eg}) &\simeq \delta_{kq} \langle \hat{a}_k^\dagger\hat{a}_k \rangle G_{\omega,n}^{MF}(\hat{\sigma}_{ge}, \hat{\sigma}_{eg}). \end{aligned} \quad (\text{A6})$$

We observe that in thermal equilibrium $\langle \hat{a}_k\hat{a}_k \rangle = \langle \hat{a}_k^\dagger\hat{a}_k \rangle \simeq 0$. Hence we conclude that the contribution of $G_{\omega,n}^{MF}(\hat{\sigma}_{ee}\hat{a}_k, \hat{\sigma}_{eg})$ to $G_{\omega,n}^{MF}(\hat{\sigma}_{ge}, \hat{\sigma}_{eg})$ can be ignored. The decoupling procedure outlined previously is equivalent to considering one-photon processes and ignoring all multiphoton contributions. Note, however, that the phonon processes are included to all orders because of the polaron transformation.

We now consider the equation of motion for $G_{\omega,n}^{MF}(\hat{\sigma}_{gg}\hat{a}_k, \hat{\sigma}_{eg})$. A similar analysis to Eqs. (A3)–(A5) yields

$$\begin{aligned} (\omega - n\Omega_0)G_{\omega,n}^{MF}(\hat{\sigma}_{gg}\hat{a}_k, \hat{\sigma}_{eg}) \\ = \omega_k G_{\omega,n}^{MF}(\hat{\sigma}_{gg}\hat{a}_k, \hat{\sigma}_{eg}) - \sum_q \tilde{\lambda}_q G_{\omega,n}^{MF}(\hat{\sigma}_{eg}\hat{a}_q\hat{a}_k, \hat{\sigma}_{eg}) \\ + \sum_q \tilde{\lambda}_q^* G_{\omega,n}^{MF}(\hat{\sigma}_{ge}\hat{a}_k\hat{a}_q^\dagger, \hat{\sigma}_{eg}). \end{aligned} \quad (\text{A7})$$

Once again the Green's functions $G_{\omega,n}^{MF}(\hat{\sigma}_{eg}\hat{a}_q\hat{a}_k, \hat{\sigma}_{eg})$ and $G_{\omega,n}^{MF}(\hat{\sigma}_{ge}\hat{a}_k\hat{a}_q^\dagger, \hat{\sigma}_{eg})$ generate equations of motion involving higher order photon operators. We decouple the two-level system and photon operators in the Green's function as before to obtain

$$\begin{aligned} G_{\omega,n}^{MF}(\hat{\sigma}_{eg}\hat{a}_q\hat{a}_k, \hat{\sigma}_{eg}) &\simeq \delta_{kq} \langle \hat{a}_k\hat{a}_k \rangle G_{\omega,n}^{MF}(\hat{\sigma}_{eg}, \hat{\sigma}_{eg}), \\ G_{\omega,n}^{MF}(\hat{\sigma}_{ge}\hat{a}_k\hat{a}_q^\dagger, \hat{\sigma}_{eg}) &\simeq \delta_{kq} (1 + \langle \hat{a}_k^\dagger\hat{a}_k \rangle) G_{\omega,n}^{MF}(\hat{\sigma}_{ge}, \hat{\sigma}_{eg}). \end{aligned} \quad (\text{A8})$$

Since in thermal equilibrium $\langle \hat{a}_k\hat{a}_k \rangle = \langle \hat{a}_k^\dagger\hat{a}_k \rangle \simeq 0$, we conclude that $G_{\omega,n}^{MF}(\hat{\sigma}_{eg}\hat{a}_q\hat{a}_k, \hat{\sigma}_{eg}) \simeq 0$ and $G_{\omega,n}^{MF}(\hat{\sigma}_{gg}\hat{a}_k, \hat{\sigma}_{eg})$ can be expressed in terms of $G_{\omega,n}^{MF}(\hat{\sigma}_{ge}, \hat{\sigma}_{eg})$ by using Eq. (A8) in Eq. (A7) as

$$G_{\omega,n}^{MF}(\hat{\sigma}_{gg}\hat{a}_k, \hat{\sigma}_{eg}) \simeq \frac{\tilde{\lambda}_k^* G_{\omega,n}^{MF}(\hat{\sigma}_{ge}, \hat{\sigma}_{eg})}{\omega - n\Omega_0 - \omega_k}. \quad (\text{A9})$$

Eliminating $G_{\omega,n}^{MF}(\hat{\sigma}_{gg}\hat{a}_k, \hat{\sigma}_{eg})$ between Eqs. (A2) and (A9) and using $G_{\omega,n}^{MF}(\hat{\sigma}_{ee}\hat{a}_k, \hat{\sigma}_{eg}) \simeq 0$, we obtain for $G_{\omega,n}^{MF}(\hat{\sigma}_{ge}, \hat{\sigma}_{eg})$ using Eq. (21):

$$\begin{aligned} (\omega - n\Omega_0)G_{\omega,n}^{MF}(\hat{\sigma}_{ge}, \hat{\sigma}_{eg}) \\ = 1 + (\omega_0 - \Delta)G_{\omega,n}^{MF}(\hat{\sigma}_{ge}, \hat{\sigma}_{eg}) \\ + \sum_k \frac{|\tilde{\lambda}_k|^2}{\omega - n\Omega_0 - \omega_k} G_{\omega,n}^{MF}(\hat{\sigma}_{ge}, \hat{\sigma}_{eg}). \end{aligned} \quad (\text{A10})$$

Solving for $G_{\omega,n}^{MF}(\hat{\sigma}_{ge}, \hat{\sigma}_{eg})$, we obtain Eq. (22).

- [1] S. John, Phys. Rev. Lett. **58**, 2486 (1987).
 [2] E. Yablonovitch, Phys. Rev. Lett. **58**, 2059 (1987).
 [3] S. John, Phys. Rev. Lett. **53**, 2169 (1984).
 [4] P. Lodahl *et al.*, Nature **430**, 654 (2004).
 [5] S. John and J. Wang, Phys. Rev. Lett. **64**, 2418 (1990).
 [6] S. John and J. Wang, Phys. Rev. B **43**, 12772 (1991).
 [7] S. John and T. Quang, Phys. Rev. Lett. **74**, 3419 (1995).
 [8] S. John and T. Quang, Phys. Rev. A **50**, 1764 (1994).
 [9] S. John and T. Quang, Phys. Rev. Lett. **76**, 2484 (1996).
 [10] S. John and T. Quang, Phys. Rev. Lett. **76**, 1320 (1996).
 [11] S. John and T. Quang, Phys. Rev. Lett. **78**, 1888 (1997).
 [12] T. Quang, M. Woldeyohannes, S. John, and G. S. Agarwal, Phys. Rev. Lett. **79**, 5238 (1997).
 [13] M. Woldeyohannes and S. John, Phys. Rev. A **60**, 5046 (1999).
 [14] M. Florescu and S. John, Phys. Rev. A **64**, 033801 (2001).
 [15] S. John and M. Florescu, J. Opt. A **3**, S103 (2001).
 [16] J. Vuckovic *et al.*, Physica E **32**, 466 (2006).
 [17] U. Hohenester, *Handbook of Theoretical and Computational Nanotechnology* (American Scientific, Valencia, CA, 2006).
 [18] B. Krummheuer, V. M. Axt, and T. Kuhn, Phys. Rev. B **65**, 195313 (2002).
 [19] L. Jacak *et al.*, Eur. Phys. J. D **22**, 319 (2003).
 [20] A. Grodecka *et al.*, e-print arXiv:cond-mat/0404364 (2004).
 [21] T. Calarco, A. Datta, P. Fedichev, E. Pazy, and P. Zoller, Phys. Rev. A **68**, 012310 (2003).
 [22] S. Schmitt-Rink, D. A. B. Miller, and D. S. Chemla, Phys. Rev. B **35**, 8113 (1987).
 [23] S. V. Goupalov *et al.*, IEEE J. Quantum Electron. **8**, 1009 (2002).
 [24] E. Pazy, Semicond. Sci. Technol. **17**, 1172 (2002).
 [25] T. Takagahara, Phys. Rev. B **60**, 2638 (1999).
 [26] T. Stauber, R. Zimmermann, and H. Castella, Phys. Rev. B **62**, 7336 (2000).
 [27] E. A. Muljarov and R. Zimmermann, Phys. Rev. Lett. **93**, 237401 (2004).
 [28] K. J. Ahn, J. Forstner, and A. Knorr, Phys. Rev. B **71**, 153309 (2005).
 [29] D. Birkedal, K. Leosson, and J. M. Hvam, Phys. Rev. Lett. **87**, 227401 (2001).
 [30] A. Ardavan *et al.*, Phil. Trans. R. Soc. Lond. B **361**, 1473 (2003).
 [31] P. Borri, W. Langbein, U. Woggon, V. Stavarache, D. Reuter, and A. D. Wieck, Phys. Rev. B **71**, 115328 (2005).
 [32] P. Borri *et al.*, Phys. Status Solidi (B) **243**, 3890 (2006).
 [33] J. Ishi-Hayase *et al.*, Appl. Phys. Lett. **88**, 261907 (2006).
 [34] P. Borri and W. Langbein, J. Phys.: Condensed Matter **19**, 295201 (2007).
 [35] R. Zimmermann and E. Runge, *Proc. 26th ICPS* (Institute of Physics, Philadelphia, 2002).
 [36] X. Q. Li, H. Nakayama, and Y. Arakawa, Phys. Rev. B **59**, 5069 (1999).
 [37] M. I. Vasilevskiy, E. V. Anda, and S. S. Makler, Phys. Rev. B **70**, 035318 (2004).
 [38] N. Vats and S. John, Phys. Rev. A **58**, 4168 (1998).
 [39] Y. Yamamoto and A. Imamoglu, *Mesoscopic Quantum Optics* (Wiley Interscience, New York, 2001).
 [40] G. D. Mahan, *Many Particle Physics* (Plenum, New York, 1990).
 [41] E. Anda and J. U. Ure, Surf. Sci. **83**, 572 (1979).
 [42] M. Weissbluth, *Photon-atom Interactions* (Academic, New York, 1989).
 [43] O. Jedrkiewicz and R. Loudon, J. Opt. B: Quantum Semiclassical Opt. **2**, R47 (2000).
 [44] D. N. Zubarev, Sov. Phys.-Usp. **3**, 320 (1960).
 [45] C. Roy, Ph.D. thesis, University of Toronto, 2009.
 [46] M. Abramowitz and I. Stegun, *Handbook of Mathematical Functions* (Dover, New York, 1972).
 [47] S. Nakajima, Y. Toyozawa, and R. Abe, *The Physics of Elementary Excitations* (Springer-Verlag, Berlin, 1979).
 [48] A. G. Kofman *et al.*, J. Mod. Opt. **41**, 353 (1994).
 [49] P. Lambropoulos *et al.*, Rep. Prog. Phys. **63**, 455 (2000).
 [50] D. Vujic and S. John, Phys. Rev. A **76**, 063814 (2007).
 [51] R. Wang and S. John, Phys. Rev. A **70**, 043805 (2004).
 [52] D. C. Langreth, Phys. Rev. B **1**, 471 (1970).
 [53] J. W. Gadzuk, Phys. Rev. B **20**, 515 (1979).
 [54] B. K. Ridley, *Quantum Processes in Semiconductors* (Clarendon, Oxford, 1999).
 [55] S. Rudin, T. L. Reinecke, and M. Bayer, Phys. Rev. B **74**, 161305(R) (2006).